Carboxymethyl Chitosan as a Selective Depressant in Differential Flotation of Galena
and Chalcopyrite

by

Yahui Xiang

A thesis submitted in partial fulfillment of the requirements for the degree of

Master of Science

in

Chemical Engineering

Department of Chemical and Materials Engineering
University of Alberta

Abstract

Toxic inorganic depressants are routinely used in the differential flotation of polymetallic sulfide ores and it is desirable that they be replaced with environmentally benign chemicals. Chitosan, as a natural and non-toxic polymer, has been proven to be an efficient depressant for copper sulfide (e.g., chalcopyrite) while allowing lead sulfide (e.g., galena) to be floated by xanthate collectors. However, the poor solubility of chitosan limits its potential applications as the flotation could only be carried out at about pH 4 where chitosan is soluble.

Three carboxymethyl derivatives of chitosan, named N-CMC, O-CMC and N-O-CMC, were synthesized by introducing carboxymethyl groups on the backbones of chitosan. The substitution on amino groups significantly improved the solubility of chitosan.

The structures of CMC were studied and compared with chitosan via Fourier transform infrared spectroscopy (FTIR) and ^{13}C nuclear magnetic resonance (NMR) spectrometry. Flotation tests were performed on single minerals and mineral mixtures (with weight ratio of 1:1) with the addition of appropriate amounts of potassium ethyl xanthate (KEX) and N-CMC. The solution pH was varied from neutral to alkaline. The flotation concentrates and tailings were collected and analysed for the contents of copper and lead.

Single mineral flotation tests indicated that N-CMC could depress either chalcopyrite or galena depending on pH. The results were not affected by the sequence of KEX and N-CMC addition. Therefore, N-CMC is potentially useful in Cu-Pb sulfide separation following a bulk Cu-Pb flotation. The N-CMC was also found to have surface cleaning functions, and was able to remove contaminating copper ions from galena surfaces.

The adsorption mechanisms of N-CMC on sulfide minerals were then delineated by several analysis techniques. Metal ions binding tests showed that N-CMC had a stronger interaction with Cu^{2+} than Pb^{2+}. The distribution of N-CMC on mineral mixtures was mapped out by time-of-flight secondary ion mass spectrometry (ToF-SIMS). The results of ToF-SIMS analysis confirmed that N-CMC preferentially adsorbed on chalcopyrite at pH 7 but uniformly distributed on both minerals at pH 10. The high resolution N 1s X-ray

photoelectron spectroscopic (XPS) spectra of N-CMC-treated chalcopyrite and galena showed that chemical bonds formed between the secondary amino groups of N-CMC and both mineral surfaces. At pH 7, the bond with Cu was stronger than with Pb, while at pH 10, one additional bond was formed between N-CMC and Pb. Zeta-potential measurements showed the presence of electrostatic interaction between N-CMC and both chalcopyrite and galena, but it was not the reason for N-CMC's selective depression of chalcopyrite.

Mineral surface cleaning tests explained the good flotation result in the absence of any chelating reagents, such as EDTA, since N-CMC also possesses the similar function of removing the Cu^{2+} adsorbed on the galena surface.

Overall, the application of N-CMC in sulfide ore flotation is expected to be more robust than the original chitosan.

Acknowledgement

Table of content

List of Figures

List of Tables

1. Introduction

In the differential flotation of complex sulfide ores, depressants are usually added to selectively prevent a certain mineral from floating. The currently used depressants in industry are mostly inorganic, such as sodium cyanide (NaCN), potassium dichromate ($K_2Cr_2O_7$) and potassium permanganate ($KMnO_4$). These inorganic depressants are very effective but also toxic and hazardous, resulting in potential harms to both human and environment. In this respect, the study on natural polysaccharide depressants, which are non-toxic and biodegradable, becomes very desirable and increasingly attracts attention (Rath & Subramanian, 1999).

For the past few decades, the research works on polysaccharide depressants have been mainly focused on starch, dextrin, carboxymethyl cellulose and guar gum. Only recently, chitosan was shown to be a selective depressant for chalcopyrite in the differential flotation of galena and chalcopyrite by Huang et al. (2012a, 2012b). Chitosan is a non-toxic polyaminosaccharide which possesses a large number of amino and hydroxyl groups. These provide active sites for the formation of metal complexes and the substitution of new functional groups (Juang et al., 1999).

Though chitosan showed good selectivity which can depress chalcopyrite without affecting the flotation of galena as recorded by Huang et al. (2012a), its depressive function was only observed at the acidic pH of 3 to 5. At higher pH, chitosan was insoluble in water and depressed both galena and chalcopyrite. This disadvantage limits its potential application as sulfide mineral flotation is usually carried out under alkaline conditions (Jayakumar et al., 2010; Wills & Napier-Munn, 2006).

The solubility of chitosan can be greatly improved by carboxymethylation (Muzzarelli, 1988). The carboxymethyl chitosan was found to have a stronger chelation ability to metal ions than the parent chitosan (Delben et al., 1989). Dobetti & Delben (1991) reported that it was the carboxyl groups and amino groups that provided sites for binding with Cu^{2+}. Muzzarelli et al. (1982) pointed out that the effectiveness of carboxymethyl chitosan as a chelation agent for metal ions was due to its bidentate functions, and the secondary and tertiary alcoholic groups present on a single polymer chain.

The main purpose of this study is, therefore, to synthesize the carboxymethyl chitosan, test its efficiency as a selective depressant in the differential flotation of chalcopyrite and galena, and investigate its adsorption mechanism on the mineral surfaces. The significance of conducting this research work is profound since it is vitally important to find effective and non-toxic replacements for inorganic depressants in the flotation industry. The new application of chitosan and its carboxymethyl derivative will also be of interest for researchers in various areas.

2. Research Objective and Approach

As mentioned in Chapter 1, the objective of this study is to investigate the efficiency and adsorption mechanism of carboxymethyl chitosan as a depressing reagent in the differential flotation of galena and chalcopyrite. Chalcopyrite and galena were chosen as they are the most common sulfide minerals coexisting in polymetallic sulfide ores. Potassium ethyl xanthate (KEX) was used as a collector. Carboxymethyl derivatives of chitosan were synthesized, and their structures were determined by Fourier transform infrared spectroscopy (FTIR), solid state ^{13}C nuclear magnetic resonance (NMR) spectroscopy and X-ray photoelectron spectroscopy (XPS). The selective depressing effect of carboxymethyl chitosan was studied in both micro and batch flotation of chalcopyrite and galena. The flotation results were further confirmed and explained by adsorption mechanism studies using photometric dispersion analysis (PDA), time-of-flight secondary ion mass spectrometry (ToF-SIMS), X-ray photoelectron spectroscopy (XPS), and zeta potential measurements. In addition, mineral surface cleaning tests were also conducted to show that carboxymethyl chitosan possesses the specific function of cleaning mineral surfaces by removing contaminating metal ions.

3. Literature review

3.1. Froth flotation

Froth flotation is a widely used separation method in the mineral processing industry with a history of about 100 years. During the flotation process, mineral particles are separated based on their different surface properties--mostly hydrophobicity. Figure 3.1 provides an illustration of a basic froth flotation process in a mechanical flotation cell. Typically, liberated mineral particles with a certain size are first agitated and mixed vigorously in the flotation cell with water. Then air is introduced from the bottom of flotation cell and generates air bubbles in the pulp. Hydrophobic particles are likely to attach to air bubbles and then levitated to the pulp surface, while most hydrophilic particles remain in the bulk. Therefore, by collecting the froth layer on top of the pulp, mineral particles with hydrophobic surfaces can be separated from those with hydrophilic surfaces.
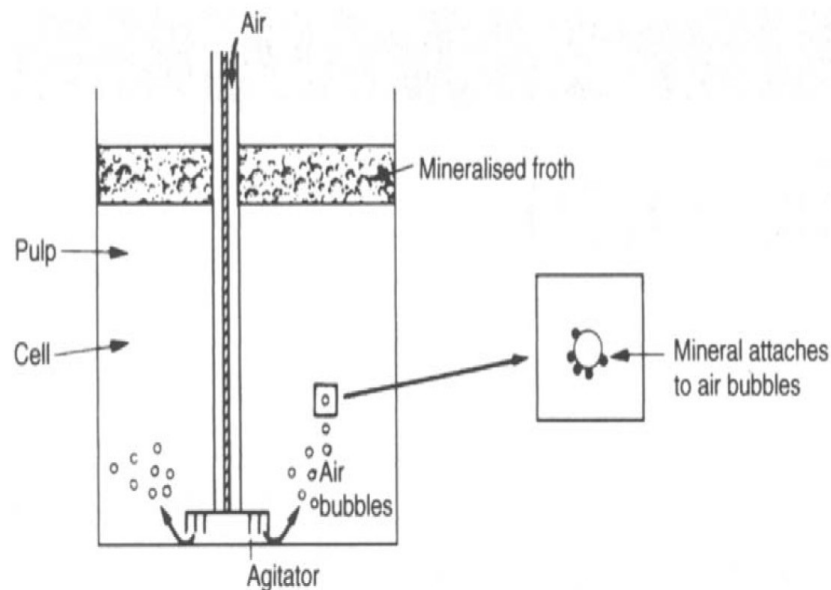
Figure 3.1 Schematics of froth flotation process (Wills & Napier-Munn, 2006)

3.1.1. Flotation reagents

Some minerals are naturally hydrophobic, such as diamonds, graphite and coal, etc., while most of the minerals are not. In order to selectively separate certain minerals, chemicals called flotation reagents are usually added in the flotation process which can modify the

hydrophobicity of mineral surfaces or change the chemical environment in flotation systems. Generally, flotation reagents are categorized into three groups: collectors, frothers and regulators. Collectors are bipolar organic reagents that can impart hydrophobicity to minerals by adsorption on mineral surfaces. Frothers are added to stabilize a froth layer and control the size of bubbles. Regulators are utilized to modify the behavior of collectors and minerals thus making the flotation process more selective. Regulators can be further classified into three types as activators, depressants and pH modifiers. Activators are specific chemical compounds that introduce hydrophobicity to the minerals by promoting collectors' interactions. On the contrary, depressants are usually used to selectively prevent certain minerals from floating by rendering them hydrophilic. The application of depressants especially organic polysaccharide depressants in differential flotation of sulfide minerals will further be discussed in Section 3.2. As indicated by the name, pH modifiers are utilized to change the pH in the flotation pulp. The change of pH can affect the flotation system in many ways. For example, surface charge of minerals can be altered under different pH conditions; ionic species and their concentrations will also be different at different pH.

3.2. Depressants in differential flotation of sulfide minerals

In the flotation of complex polymetallic sulfide ores, depressants are usually added to selectively render given minerals hydrophilic thus achieving the isolation of individual minerals (Bulatovic & Wyslouzil, 1995). For example, with xanthate as a collector, it is possible to separate galena (PbS) from chalcopyrite ($CuFeS_2$) using sodium cyanide as the depressant. Unlike xanthate which interacts with both sulfides, the depression effect of sodium cyanide only works on chalcopyrite with no interference with the flotation of galena.

There are several ways by which depressants prevent minerals from floating in differential flotation, some of which are listed below:

(1) Depressants can remove the coating of collectors from mineral surfaces, resulting in depression of the mineral.

(2) Depressants are capable of reacting with mineral surfaces directly, causing the change of composition on mineral surfaces. In this way, they can prevent the adsorption of collectors on the mineral surface entirely.

(3) Some depressants also have the ability to depress certain minerals no matter how well the latter react with collectors. By adsorbing on the mineral surface, these depressants create a hydrophilic film on the surface rendering the mineral non-floatable.

Depressants can be simply classified into two types: inorganic depressants and organic depressants. The most widely used depressants in industry are usually inorganic. Some inorganic depressants and their applications in differential flotation of sulfide minerals are given in Table 3.1.

Table 3.1 Some inorganic depressants and their primary functions in differential flotation of sulfide minerals (Pearse, 2005)

Typical inorganic depressants used in differential flotation of sulfide minerals	Primarily used as the depressant for
Cyanide (NaCN and KCN)	Pyrite and sphalerite
Zinc sulfate ($ZnSO_4$)	Sphalerite
Sodium sulfite (Na_2SO_3)	Pyrite, sphalerite and oxidised galena
Ammonium sulfate ($(NH_4)_2SO_4$)	Sphalerite
Dichromate ($K_2Cr_2O_7$, $Na_2Cr_2O_7$)	Galena
Potassium permanganate ($KMnO_4$)	Most sulfide minerals including sphalerite, pyrrhotite and chalcopyrite

Obviously, most of the aforementioned inorganic depressants are toxic and hazardous, whose uses are more and more restricted with the increasing concern of environmental issues. This results in a growing interest of investigating effective organic depressants as replacements for toxic depressants (Liu & Laskowski, 1989a).

Most of the organic depressants are naturally derived polysaccharides composed of monosaccharides (sugar) units (Liu et al., 2000). Based on their polar groups, these polysaccharide depressants can be further divided into four major groups: a) Non-ionic,

which contain hydrolyzing polar groups -OH, C=O; b) anionic, containing anionic groups, -COOH, -SO₃H, -OSO₃H; c) cationic, containing cationic groups, -NH₂, =NH; d) amphoteric with both anionic and cationic groups (Bulatovic, 1999). Starch, dextrin and guar gum are usually considered to be non-ionic polysaccharides, while they also have slight anionic character (Pugh, 1989a). Carboxymethyl cellulose is the representative polysaccharide depressant with anionic groups.

Studies on the use of polysaccharides in the differential flotation of sulfide minerals are limited (Laskowski et al., 1991). In 1957, Dolivo-Dobrovoskii and Rogachevskaya did a series of experiments on the separation of ZnS (sphalerite)-PbS (galena) and PbS-CuFeS₂ (chalcopyrite) mixtures using water-soluble starch as the depressant. Their laboratory results showed that in neutral pH, starch depressed chalcopyrite and sphalerite while galena was floated (Dolivo-Dobrovoskii & Rogachevskaya, 1957). However, starch, dextrin and guar gum are more widely used as depressants for galena in differential flotation of chalcopyrite and galena, and mostly together with sulfuric acid or sulfur dioxide (Schnarr, 1978; Allan & Bourke 1978; Lin & Burdick 1988). By adjusting the pulp pH and changing the addition sequence of reagents, dextrin can be used as the depressant for either galena or chalcopyrite under different conditions. As reported by Liu and Laskowski (1989), when xanthate was used as the collector and added prior to dextrin, galena was depressed around pH 12 while chalcopyrite was floated; when dextrin was added prior to xanthate, chalcopyrite was depressed around pH 6 while galena was floated from the mixture (Liu & Laskowski, 1989a).

Modification to polysaccharides can be made by introducing different functional groups through etherification or esterification reactions with hydroxyl groups (Liu et al., 2000). A typical example is carboxymethyl cellulose, with the protons in some hydroxyl groups being replaced by carboxymethyl groups. Carboxymethyl cellulose is extensively used as a depressant for hydrophobic gangue and silicate minerals in Cu-Ni sulfide flotation. Bakinov et al. (1964) studied the relationship between the structure of carboxymethyl cellulose and its depression performance in the flotation of nickel ores. It was found that, by using carboxymethyl cellulose with high levels of polymerization and a low degree of substitution, the nickel content in the concentrate was greatly improved. In another work,

carboxymethyl cellulose was used as a depressant for galena under alkaline condition, whereas Cu-activated sphalerite was floated from the concentrate (Jin et al., 1987). As pointed out by their results, under alkaline pH, carboxymethyl cellulose was more likely to adsorb on galena than sphalerite, due to their chemical bonding to galena rather than only hydrogen bonding with sphalerite. The adsorption mechanism between polysaccharide depressants and minerals will be further discussed in the next section.

3.3. Adsorption mechanism

The adsorption mechanism between polysaccharides and minerals is very different from collector adsorption and other inorganic reagents adsorption. The type and steric configuration of functional groups, molecular weight and charge density, etc., all contribute to the adsorption behavior of polysaccharides (Bulatovic, 2007). However, the limited application of polysaccharides in mineral processing and the lack of a thorough understanding of polysaccharides adsorption mechanism on minerals mutually hinder the development of each other (Liu et al., 2000). Currently, the most widely proposed adsorption mechanisms between polysaccharides and minerals are: hydrogen bonding, hydrophobic interaction, chemical complexation and electrostatic interactions. The standard free energy for the adsorption ($\Delta G°_{ads}$) of a polysaccharide on the mineral-solution interface can be expressed by adding up the standard free energies of these four contributions:

$$\Delta G°_{ads} = \Delta G°_{h-bond} + \Delta G°_{phobic} + \Delta G°_{chem} + \Delta G°_{elec} \qquad （3\text{-}1）$$

The sign and magnitude of each aforementioned term depend on the surface properties of minerals and the characteristics of polysaccharides, and vary with different mineral-polysaccharide pairs (Jenkins & Ralston, 1988).

3.3.1. Hydrogen bonding

Hydrogen bonding is essentially an electrostatic dipole-dipole attraction which is formed when hydrogen is bound with highly electronegative elements (usually F, N, O) or highly

electronegative groups such as $-CN$, $-CCl_3$. The strength of hydrogen bonding is much weaker than covalent bonds but stronger than other dipole forces (Israelachvili, 2011).

In many early studies, hydrogen bonding is suggested to be the primary adsorption mechanism between polysaccharides and minerals without any direct proof (Balajee and Iwasaki, 1969; Hanna, 1973; Afenya, 1982). These hypotheses were mainly focused on the hydroxyl groups in polysaccharides and assumed that they can form hydrogen bonds with the hydroxyl groups on mineral surfaces. However, if hydroxyl groups in aqueous solutions are considered, they would have formed hydrogen bonds with minerals and polysaccharides already before new hydrogen bonding occurs between minerals and polysaccharides. In this case, the formation of a new hydrogen bond requires the breakdown of at least two existing hydrogen bonds, while the energy involved in this process has remained unstudied. Taking hydrogen bonding alone as the adsorption mechanism in aqueous solutions is then regarded as questionable (Liu & Laskowski, 2002).

3.3.2. Hydrophobic interaction

The occurrence for hydrophobic interaction is usually due to the tendency of non-polar groups on polymer chains to adhere with other non-polar species in a polar aqueous environment (Nemethy & Scheraga, 1962).

Dextrin was found out to have an exclusive preference for naturally hydrophobic minerals, such as talc, graphite, molybdenite and coals in its early applications. The "hydrophobicinteraction" was thus proposed as the adsorption mechanism for dextrin on mineral surfaces (Wie and Fuerstenau, 1974; Haung et al 1978; Afenya, 1982). In the study of Miller et al. (1983), evidences of hydrophobic interaction were given, based on the increasing dextrin adsorption with the increasing hydrophobicity on coal surfaces. Another proof for hydrophobic interaction from a different perspective was provided by Beaussart et al. (2009). In their study, dextrin adsorbed more significantly on graphite than on molybdenite and talc when these three minerals have similar surface hydrophobicities. They believed that the hydrophobic interaction between dextrin and graphite was enhanced by their closer geometric match.

In addition to dextrin, other polysaccharide depressants like carboxymethyl cellulose were also believed to adsorb on minerals through hydrophobic interaction (Morris et al., 2002).

3.3.3. Chemical complexation

The adsorption between polysaccharides and minerals had long been attributed to hydrogen bonding and hydrophobic interaction, while experimental evidences for chemical complexation were increasingly recorded (Liu et al., 2000). Somasundaran (1969) studied the adsorption of starch on calcite and proposed that a chemical complex formed between starch and calcium species at the surface. His hypotheses was based on the fact that, by adding starch to calcite suspension, there was an increase in the amount of calcium ions in the solution. A similar phenomenon was reported by Khosla et al. (1984), in whose work, there was a positive discrepancy (increase) in the conductivity of both Fe^{3+}/starch and Ca^{2+}/starch systems. Besides, in their infrared spectra for the mixture of starch or starch fraction (amylose and amylopectin) and Fe_2O_3 or Fe^{3+}, new adsorption bands at 1200 cm^{-1} were observed, which was ascribed to the chemical interaction between Fe_2O_3 or Fe^{3+} with starch or starch fractions. These two studies above did draw attention to chemical complexation, but neither of them shed any light on how the chemical complex was formed.

Liu and Laskowski (1989b) did a series of IR measurements on the precipitates formed in dextrin/lead nitrate solutions of different dextrin-lead ratios. They found that the peaks of dextrin between 1000 and 700 cm^{-1} gradually disappeared when the ratio of dextrin-lead decreased from 5:1 to 1:1 to 1:5. The peaks at 930 and 760 cm^{-1} were related to asymmetric and symmetric deformation of the glucose ring which can be strongly influenced by the substitution on hydroxyl groups. They believed that the weakening and disappearance of these peaks were due to the strain placed on the glucose ring after chemical bonding formed between lead ions and hydroxyl groups on C-2 and C-3. In their summary, they proposed a five-member ring complex (as shown on Figure 3.2) formed on the lead hydroxide surface to explain the interactions between dextrin and lead.
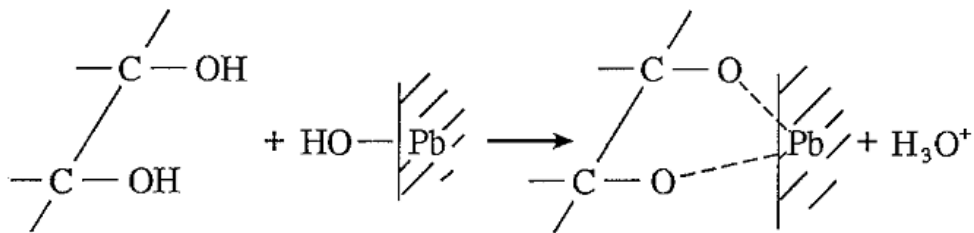
Figure 3.2 The five-membered ring complex between dextrin and lead proposed by Liu & Laskowski, 1989b

Later, a very similar complexation model was proposed by Weissenborn et al. (1995). They used diffuse reflectance infrared Fourier transform spectroscopy (DRIFTS) to study the adsorption of wheat starch amylose and amylopectin on hematite. The major changes of adsorbed wheat starch, amylose and amylopectin after their adsorption on hematite were the shifts of glucopyranose ring vibration and C_1-H deformation. These observed shifts indicated that an eight-membered ring complex formed between polysaccharide hydroxyl groups attached to C-2 and C-3 and surface iron atoms from hematite (Figure 3.3).
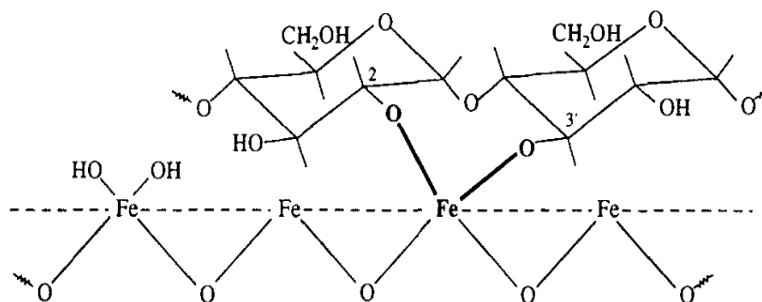
Figure 3.3 The eight-membered ring complex between starch or starch fraction (amylose and amylopection) and hematite proposed by Weissenborn et al., 1995

3.3.4. Surface charge, electrical double layer and zeta potential

In aqueous solutions, solid surfaces can be charged for many reasons which include: the preferential dissolution of surface species, hydrolysis and ionization of surface species, adsorption of various charged ions and complexes (Somasundaran & Wang, 2006).

In terms of oxide minerals and silicates in aqueous solutions, the charge on mineral surfaces is mainly due to the hydrolysis of surface species followed by pH-dependent dissociation of surface hydroxyl groups (Fuerstenau et al., 2007):

$$MOH = MO^- + H^+ \qquad\qquad (3\text{-}2)$$

$$H^+ + MOH = MOH^+ \qquad\qquad (3\text{-}3)$$
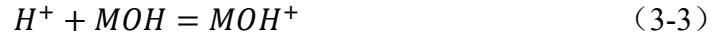
The pH-dependent dissociation of oxide minerals was also illustrated by Fuerstenau and Fuerstenau (1982) as:
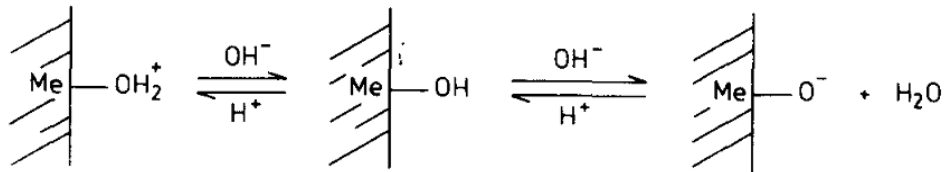
Figure 3.4 The dissociation of oxide minerals in aqueous solutions (Fuerstenau & Fuerstenau, 1982)

M and Me in the equations and schematic above both represent the interfacial metal atom.

The surface charge of oxide minerals in aqueous solution can therefore be controlled by pH. At a specific pH, the surface charge is zero, and this pH value is called point-of-zero-charge, PZC. Oxide minerals will be positively charged in the solutions with lower pH than PZC, while in the solutions that are more alkaline than PZC, they can be negatively charged (Fuerstenau et al., 2007).

Once the solid surface gets charged, a potential will be introduced between the solid surface and aqueous phase. Ions in the surrounding solution will be redistributed to neutralize the surface charge on the solid surface and leads to the electrical double layer. Basically, the electrical double layer consists of a Stern layer which formed by the surface charge together with the adsorbed counter ions, and a diffuse layer which is an atmosphere of ions in rapid thermal motion close to the surface. The ions at diffuse layer have more freedom compared to the bound ions in the Stern layer. (Israelachvili, 2011; Graham, 1947).
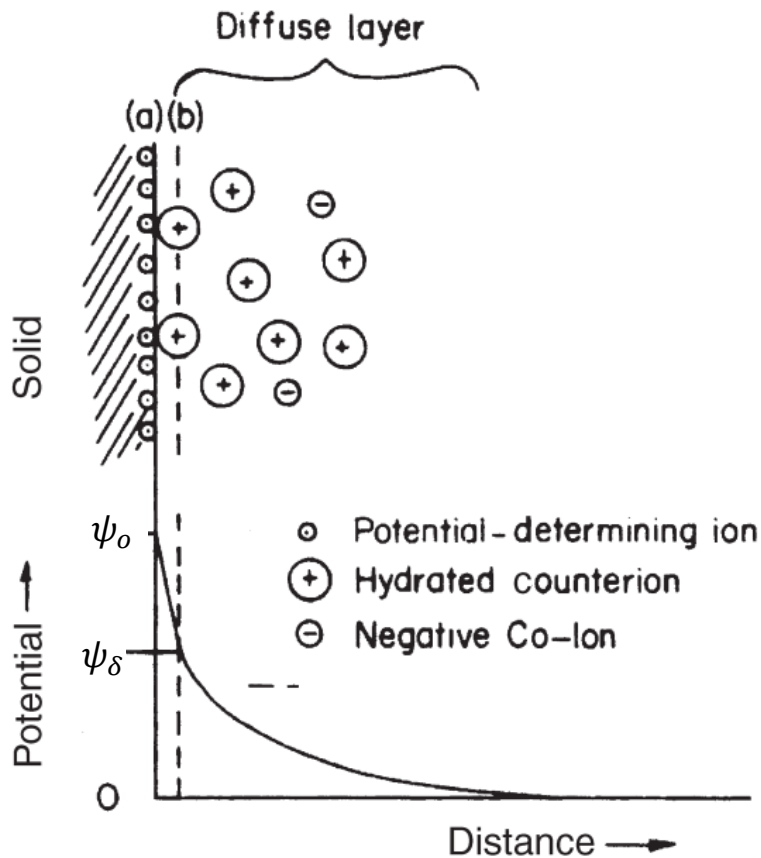
Figure 3.5 Schematic representation of the Gouy-Chapman electrical double layer and potential drop across the double layer (Fuerstenau et al., 1985)

A schematic representation of the Gouy-Chapman electric double layer and potential drop across the double layer are shown in Figure 3.5. Ions involved in the double layer can be classified into three parts: a) the potential-determining ions at the mineral surface; b) a layer of counter ions adsorbed on the mineral surface; c) counter ions in the surrounding solution which form a diffuse layer. In Gouy-Chapman's model, the potential decreases exponentially as a function of distance away from the surface. The total double layer potential or surface potential is ψ_o, the potential at the Stern layer where the closest counter ions locate is called ψ_δ, and the potential at shear plane or slipping plane is called the zeta potential (ζ). Since it is not possible to measure the surface potential ψ_o directly, the electrokinetic behavior of mineral particles and adsorption phenomena in flotation are usually characterized by zeta potential measurements (Fuerstenau et al., 1985). The pH

value where the zeta potential is zero, is called the isoelectric point (i.e.p.). The i.e.p and PZC are often used interchangeably; however, they indeed have different values when there is specific adsorption on the mineral surface.

3.3.5. Electrostatic interactions

Depending on the charges on mineral surfaces and on the polysaccharide chains, the attractive or repulsive electrostatic interactions can take place with the free energy given by:

$$\Delta G_{elec} = zF\psi_\delta \qquad\qquad (3\text{-}4)$$

where z is the valency of the adsorbate species, F is the Faraday constant, and ψ_δ is the potential at the δ plane where the polysaccharide head group is located (Fuerstenau et al., 2007).

As discussed in section 3.2, carboxymethyl cellulose is an anionic polysaccharide, while starch, dextrin and guar gum are non-ionic. However, the non-ionic polysaccharides can also obtain surface charge by the introduction of anionic or cationic species. Furthermore, the ionization of impurities or hydroxyl groups in these polysaccharides can also render their surface charged (Foster et al., 1965).

Somasundaran (1969) proposed that there was an attractive electrostatic interaction between the negatively charged starch and positive sites on calcite. His hypothesis was based on the previous studies about the negative charge on starch (Taylor and Iddles, 1926; Frahn and Mills, 1959) and further supported by the negative shifts in the zeta potential measurement of calcite in aqueous solutions after the addition of starch.

Bicak et al. (2007) studied the adsorption of guar gum and carboxymethyl cellulose on pyrite, and found that, unlike guar gum, carboxymethyl cellulose did not adsorb effectively on pyrite. In addition, they also observed that the adsorption density of carboxymethyl cellulose with a low substitution degree (with less anionic carboxymethyl groups) on pyrite is higher than the highly substituted one (with more anionic carboxymethyl groups). The main reason was the repulsive electrostatic interactions between the negatively charged groups on carboxymethyl cellulose and the negatively charged pyrite.

3.3.6. Surface activation or contamination of sulfide minerals

The surface activation or contamination is a specific phenomenon in sulfide minerals flotation, especially in the case of zinc sulfide flotation. In practice, zinc sulfide does not float effectively with xanthate collector, since the products that are formed by the collector, such as zinc xanthate, are comparatively soluble in aqueous solutions, and fail to render the zinc sulfide surface hydrophobic (Wills & Napier-Munn, 2006). When the flotation of zinc sulfide is desired, surface activation can be realized by adding metal ions whose sulfides are more insoluble. By far, Cu(II) is the most commonly used metal ion as the activator for zinc sulfide, while Pb(II), and Fe(II/III) are also found to improve the floatability of zinc sulfide or other minerals (Fornasiero & Ralston, 2006). A thorough review about the activation of sulfide minerals in flotation and another review about the activation mechanism were given by Finkelstein (1997) and Chandra and Gerson (2008), respectively.

However, in the differential flotation of sulfide minerals, the selectivity can also be reduced due to the unwanted activation effect, i.e., surface contamination. The unintentional surface contamination caused by metal ions or metal hydroxides can be removed by using chelating reagents, such as EDTA (ethylenediaminetetraacetic acid).

3.4. Chitosan

3.4.1. Structure and property of chitosan

Chitosan is a polyaminosaccharide produced from the deacetylation of chitin (Wan Ngah et al., 2011). Chitin, as the second most abundant polysaccharide in nature after cellulose, exists predominately in the shells of crustaceans, such as crabs, shrimps, and lobsters (Pillai et al., 2011; Kittur et al., 2002). Figure 3.6 shows the structure of cellulose, chitin, and chitosan. As can be seen, chitin has a similar structure to cellulose, and can be regarded as cellulose with hydroxyl groups on C-2 substituted by acetamido group (Kumar, 2000). The high percentage of N (6.89%) in the structures of chitin and chitosan compared to synthetically modified cellulose (1.25%) is their main reason for winning commercial interest (Kumar, 2000). For chitosan, the primary and secondary hydroxyl groups and

amino groups on the glucosamine provide active sites for the formation of metal complexes and the substitution of new functional groups (Zeng et al., 2008; Pillai et al., 2011). With the presence of amino groups, chitosan can be cationized in acidic environment, and is then able to adsorb on anionic surfaces by electrostatic interactions (Zeng et al., 2008). As the N-deacetylated products of chitin, only those with the degree of deacetylation greater than 50% can be considered as chitosan (Pillai et al., 2011). However, the deacetylation of chitin is almost never complete, and there will always be some residual acetyl groups on chitosan (Varma et al., 2004). Therefore, chitosan is indeed a copolymer of glucosamine and N-acetyl glucosamine (Figure 3.7). The degree of deacetylation (DA) of chitosan has been studied and examined by many analytical instruments, including IR spectroscopy, ^{1}H NMR and ^{13}C solid state NMR, UV spectrophotometry, etc., and more recently by near-infrared spectroscopy (Jayakumar et al., 2010).

As the major component of crustaceans shells, chitin is extremely hydrophobic and insoluble in water and most organic solvents, while only a few solvents are applicable for its dissolution, such as hexafluoroisopropanol, hexafluoroacetone and chloroalcohols with mineral acids in aqueous solutions. Chitosan can be dissolved in dilute aqueous acids, such as acetic acid and formic acid (Kumar, 2000).

The molecular weight (M) of chitosan can be determined rapidly by the viscometry method through the Mark-Houwink equation:

$$[\eta] = KM^{\alpha} \qquad\qquad （3\text{-}5）$$

where $[\eta]$ is the intrinsic viscosity, and the constants K and α depend on the particular polymer-solvent system.

However, attention should be paid when choosing these constants, due to the cationization and aggregation of chitosan in dilute acid (Pillai et al., 2011). The weight-average molecular weight (M_w) of chitosan can be determined by light scatting (Muzzarelli et al., 1987). The M_w for chitin is 1.03×10^6 to 2.5×10^6, while for chitosan is 1×10^5 to 5×10^5 (Lee, 1974).
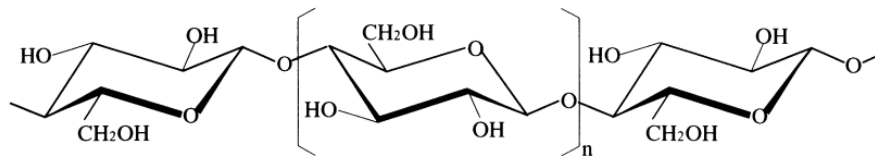
(a)
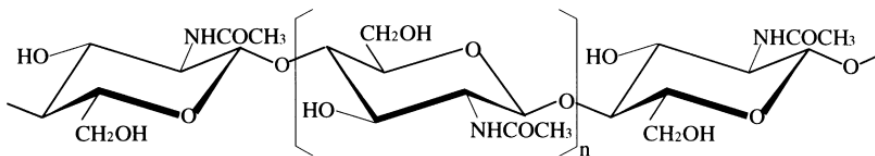
(b)
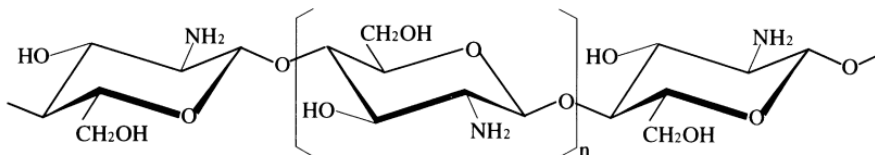
(c)

Figure 3.6 Chemical Structure of: a) cellulose, b) chitin and c) chitosan (Okuyama et al., 2000)
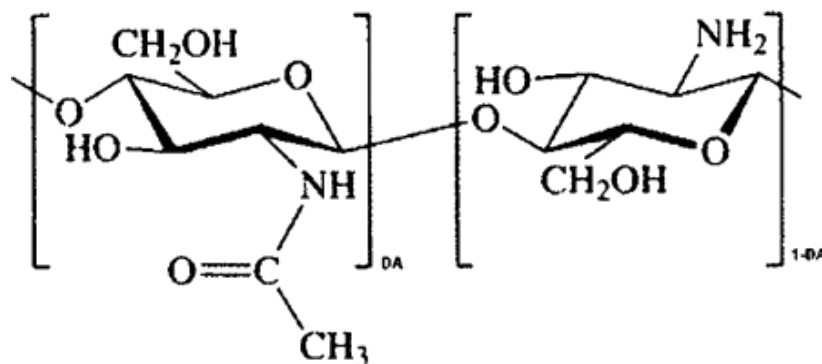
Figure 3.7 Structure of incompletely deacetylated chitosan, a copolymer characterized by its average degree of deacetylation (DA) (Dutta et al., 2004)

3.4.2. Carboxymethylation of chitosan

With the presence of amino groups, primary and secondary hydroxyl groups, chitosan can be modified through chemical reactions. The carboxymethylation is one of the most widely-studied modifications for chitosan, which can introduce carboxymethyl groups ($-CH_2$-COOH) onto chitosan. Since there is more than one reactive site in chitosan's molecular structure, three carboxymethyl derivatives with different substitution sites, i.e., O-CMC (with –OH being substituted), N-CMC (with $-NH_2$ being substituted), N-O-CMC (with both –OH and $-NH_2$ being substituted), can be prepared through different synthesis routes (Kong, 2012). A thorough and detailed review about the synthesis procedures of carboxymethyl chitosans was provided by Muzzearelli in 1988.

These three carboxymethyl derivatives of chitosan are named as CMC (carboxymethyl chitosan) in general and share some properties in common including:

1. Water-soluble: One of the most desirable characters for chitosan's derivatives is the good solubility in aqueous solutions, and this can be realized by introducing hydrophilic carboxymethyl groups in chitosan's structure (Mourya et al., 2010). It has been experimentally proved that CMC can become soluble in aqueous solutions in the entire pH range, though a minimum DS (degree of substitution) may be required (Chen et al., 2003; Tungtong et al., 2012).

2. Amphoteric: Chitosan is a cationic polysaccharide because of the positively charged amino groups in acidic solutions. The introduction of carboxymethyl groups can render chitosan amphoteric which contains both cationic and anionic groups. The ionic strength as well as the adsorption behaviour of CMC can, therefore, be controlled by the DS of carboxymethyl groups or pH values (Tiwary et al., 2011).

3. Strong chelation ability: Chitosan itself is an excellent selective chelating reagent for transition metals, such as Ag, As, Cu, Co, Fe, Hg, Mo, Ni, Pb (Mourya et al., 2010). The strong chelation ability of chitosan is mainly attributed to $-NH_2$ groups which can form chemical complexation with metal ions through either a "bridge" or a "pendent" method (Nieto et al., 1992; Ogawa et al., 1993). N-CMC and N-O-CMC are shown to adsorb more Fe^{3+}, Co^{2+}, Cu^{2+}, Pb^{2+}, Ni^{2+}, Cd^{2+} ions than chitosan

(Wang et al., 2008; Delben et al., 1989; Delben & Muzzarelli, 1989), and their enhanced chelation ability can be ascribed to the –NH-CH$_2$-COOH (glycine) group which was found to enable the formation of pentaatomic rings in metal chelates (Muzzarelli et al., 1982). Besides, the carboxyl groups which exist in all CMC structures also contribute to their high chelation abilities. In the study by Muzzarelli (1988), a typical adsorption band for the charge transfer from carboxylate to copper was observed on the IR spectrum of O-CMC/copper chelate, which indicated that Cu^{2+} ions were mainly bound to COO$^-$ groups.

3.4.3. Application of chitosan and its derivatives

Chitosan is a natural cationic polysaccharide with large numbers of hydroxyl groups and amino groups. It shows many advantages over artificial materials such as biodegradability, biocompatibility, non-toxicity, and adsorption properties (Kumar, 2000). In addition to these advantages that are inherited from the parent chitosan, carboxymethylated chitosan (CMC) also possesses good solubility and amphoteric properties. Both chitosan and CMC have been extensively tested in various areas which include: biomedical & pharmaceutical fields (Dash et al., 2011; Upadhyaya et al., 2013; Jayakumar et al., 2010); water & waste treatment (Bhatnagar & Sillanpää, 2009; Wan Ngah et al., 2011; Chattopadhyay & Inamdar, 2014; Zeng et al., 2008); battery industry (Morni & Arof, 1999; Subban & Radhakrishna, 1996; Yue et al., 2014); cosmetics (Hirano et al., 1991; Chen et al., 2006); and food industry (Shahidi et al., 1999; Dutta et al., 2009).

The application of chitosan in mineral flotation was never discussed earlier until recently. Huang et al. reported a series of research works on using chitosan as a depressing reagent in the differential flotation of sulfide minerals. Their motivation was to find a non-toxic and environmentally friendly alternative to the currently used inorganic and toxic depressants in sulfide mineral flotation. In their first study of chitosan in 2012 (Huang et al., 2012a), chitosan was exploited as the depressant in the differential flotation of chalcopyrite (CuFeS$_2$) and galena (PbS) with potassium ethyl xanthate (KEX) as a collector. It was observed that, in the mixed mineral flotation, galena was floated while chalcopyrite was selectively depressed by chitosan. However, this depressive effect only occurred at acidic conditions between pH 3 and 5. The best result was observed at pH 4 where the

recovery for galena was 95% while only 30% for chalcopyrite. The adsorption mechanism between chitosan and Cu and Pb sulfide minerals was investigated by adsorption isotherms and XPS measurements in this paper, and further studied by FTIR and ToF-SIMS in their subsequent work (Huang et al., 2012b). Through the adsorption density study, it was shown that Cu^{2+} ions exhibited higher affinity to chitosan than Pb^{2+} ions. The ToF-SIMS images together with elemental maps showed that chitosan's image matched the pattern of chalcopyrite instead of galena, which indicated chitosan mainly adsorbed on chalcopyrite. XPS and FTIR analysis revealed the fact that the amino groups and hydroxyl groups on chitosan took active part in the strong interaction with chalcopyrite, while chitosan-galena interaction was more likely a hydrophobic interaction through the acetyl units of chitosan. In this respect, chitosan with a complete degree of deacetylation (DA) would be a highly selective depressant in Cu-Pb sulfide mineral flotation. Later on, they continued the study of chitosan as a depressing reagent in the differential flotation of galena (PbS) and sphalerite (ZnS) with KEX as a collector (Huang et al., 2013a), followed by the differential flotation of galena (PbS) and pyrite (FeS_2) using chitosan as a depressant as well (Huang et al., 2013b). Sphalerite was selectively depressed by chitosan while galena was floated at pH 4, with either the addition of EDTA or pre-coating sphalerite by Cu^{2+} ions. Pyrite was selectively depressed (23% recovery) by chitosan while galena was floated (68% recovery) at pH 4. In both of these flotation studies, amino groups and hydroxyl groups on chitosan were found to be involved in the interaction with minerals that were depressed, through a chemisorption mechanism, while the weak interaction between chitosan and galena was attributed to physisorption. Based on the preferential adsorption of chitosan on chalcopyrite, sphalerite and pyrite over galena, they assumed that it was due to the tendency of the amino groups on chitosan to bind with metal ions that have a higher electron affinity. Among all these studies about chitosan in differential flotation of sulfide minerals, the selectivity of chitosan as a depressant was indeed observed but only under acidic pH condition. The low pH range is, however, not suitable for sulfide mineral flotation processes, especially when the flotation is carried out on a large scale, since most collectors including xanthates are stable under alkaline condition and corrosion of cells and pipelines also need to be minimised (Wills & Napier-Munn, 2006). The application of using chitosan as a depressant in the flotation industry is, therefore, hindered.

Inspired by Peng Huang's work, efforts on utilizing chitosan's derivative as a depressant in oxide mineral flotation were later made by Wang and Liu (2013). Phosphorylated chitosan was synthesized and structural analyses showed that during the synthesis procedure, methanesulfonic acid was ionically bound to the amino groups of chitosan, and the phosphate groups were grafted on C-6 hydroxyl sites on chitosan. The chemical structure of phosphorylated chitosan can be seen from Figure 3.8. Single mineral flotation tests were carried out on rhodochrosite ($MnCO_3$) and malachite ($Cu_2CO_3(OH)_2$) by using phosphorylated chitosan as depressant and sodium oleate as a collector. The results indicate that the depressive function of phosphorylated chitosan was observed on both minerals but at different pH: for rhodochrosite it was at pH 7 to 11, and for malachite it was only at pH 7. FTIR and XPS analyses revealed the adsorption mechanism, that the strong interaction between phosphorylated chitosan and rhodochrosite was attributed to the covalent bonds of both P=O and P-OH groups with rhodochrosite, while for malachite only P-OH was involved in the adsorption through hydrogen bonding.
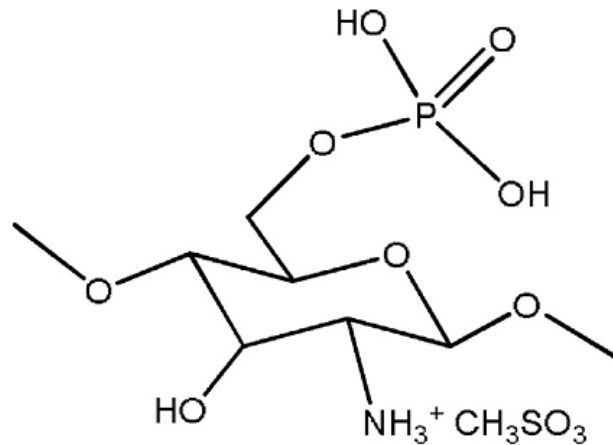
Figure 3.8 The chemical structure of phosphorylated chitosan using methanesulfonic acid as a blocking agent. The product has nitrogen, phosphorous and sulfur (Wang & Liu, 2013)

4. Experimental

4.1. Mineral samples

Natural chalcopyrite (originated from Durango, Mexico) and galena (mined from Moroco) minerals were purchased from Ward's Scientific Establishment. Chemical compositions of the two mineral samples were measured by X-ray diffraction (XRD) and no impurities except quartz were found in chalcopyrite. According to XRD and elemental analyses, the purity of chalcopyrite was 84.5% (containing 29.26% Cu), and the purity of galena was 97% (containing 84% Pb). The lumps of chalcopyrite and galena were crushed by a Retsch Jaw Crusher (Retsch, USA), then ground in a mechanized mortar/pestle grinder (Fritsch Mortar Grinder Pulverisette 2, Germany) to collect the desired fractions. The -75+45 μm and -200+150 μm fractions were respectively used in micro-flotation test and batch flotation test. The mineral particles of -20 μm were used in adsorption tests, and their specific surface areas were analyzed by BET method. The specific surface area was 1.391 m^2/g for the -20 μm chalcopyrite and 0.390 m^2/g for the -20 μm galena.

The ground quartz (>99.5% SiO_2) that was used in batch flotation tests was purchased from U.S. Silica. It was produced from high purity silica powder, and precision ground down to the top size of 90 μm.

4.2. Reagents and chemicals

Chitosan (MW 100,000-300,000, degree of deacetylation >90%) was purchased from ACROS Organics Canada Inc. Glyoxylic acid, sodium borohydride and chloroacetic acid were purchased from Sigma-Aldrich Canada Inc. All other reagents used in this study, such as acetic acid, sodium hydroxide, hydrochloric acid, acetone, ethanol, cupric sulfate and lead nitrate, were of pure analytical grade purchased from Fisher Scientific Canada. The KBr powder used in FTIR analysis was of spectroscopic grade purchased from PIKE Technologies, USA.

Commercial-grade potassium ethyl xanthate (KEX) was obtained from Prospec Chemicals Ltd., Canada and was purified by multiple recrystallization from acetone. Hydrochloric

acid and sodium hydroxide (Fisher Scientific Canada) were used to adjust pH. All the aqueous solutions used throughout the study were prepared using distilled water.

4.3. Carboxymetylation of chitosan

4.3.1. Synthesis of N-carboxymethyl chitosan (N-CMC)

The synthesis reaction of N-CMC is shown in Figure 4.1 and the procedure was adopted from the preparation process by Muzzarelli et al. (1982) with modification. The detailed procedure is as follows:

1. Dissolve 1 g chitosan in 50 mL 1% acetic acid to prepare a chitosan acetate solution.

2. Add 1.72 g glyoxylic acid and stir for 1.5 hours under room temperature.

3. Adjust pH to 10 by adding 10% sodium hydroxide solution drop wise.

4. Then gradually add 0.69 g sodium borohydride and stir for 1.5 hours in an ice bath.

5. Pour the solution into vigorously stirred anhydrous ethanol solution. A white precipitate is immediately formed.

6. Filter the precipitate and further rinse it with anhydrous ethanol for three times.

7. Vacuum dry the product overnight.

The final N-CMC product shows excellent solubility in water. It dissolves well under any pH.
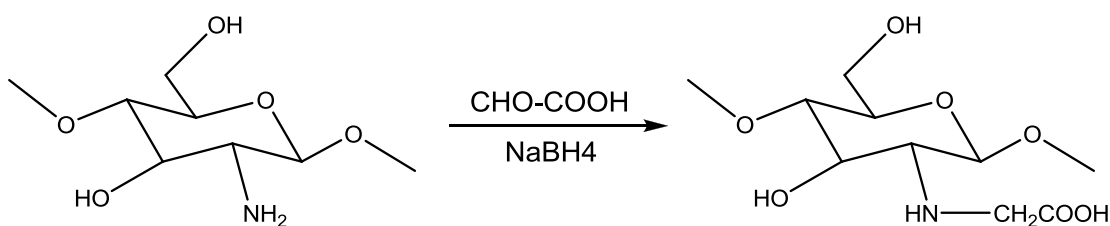
Figure 4.1 The synthesis reaction of N-CMC (Muzzarelli et al., 1982)

4.3.2. Synthesis of O-carboxymethyl chitosan (O-CMC)

The synthesis reaction of O-CMC is shown in Figure 4.2, and the procedure was based on the method of Muzzarelli (1988) with modifications:

The first three steps are the same as the synthesis of N-CMC.

4. Gradually add 5 g chloroacetic acid and stir for 1.5-2 hours in a 60 ℃ water bath.

5. After reaction, pour the solution into a vigorously stirred anhydrous ethanol solution.

5. Filter the precipitate and vacuum dry.

6. Add the raw product from the previous step into 1% hydrochloric acid solution and stir for 1 hour.

7. Pour the solution again into anhydrous ethanol, filter the precipitate and rinse three times with anhydrous ethanol.

8. Vacuum dry the product overnight.

The final product of O-CMC is hardly soluble in water.
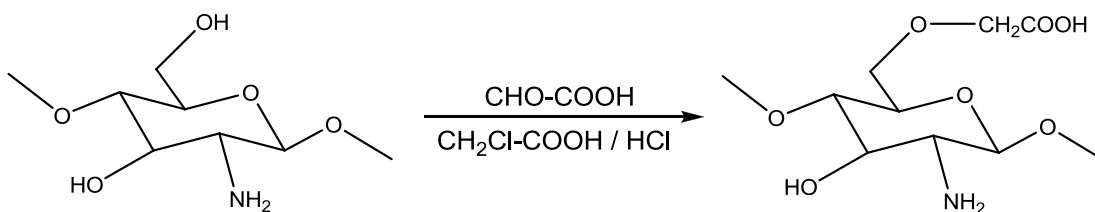
Figure 4.2 The synthesis reaction of O-CMC

4.3.3. Synthesis of N-O-carboxymethyl chitosan (N-O-CMC)

The synthesis reaction of N-O-CMC is shown in Figure 4.3. The procedure was based on Hayes (1986) but greatly simplified:

The first four steps are the same as the synthesis of O-CMC.

5. Allow the solution to cool to room temperature after reaction.

6. Gradually add 0.69 g sodium borohydride and stir for 1.5 hours in an ice bath.

7. After the reaction, pour the solution into vigorously stirred anhydrous ethanol, filter the precipitate and rinse with anhydrous ethanol for three times.

8. Vacuum dry the product overnight.

The final product of N-O-CMC shows a good solubility in water.
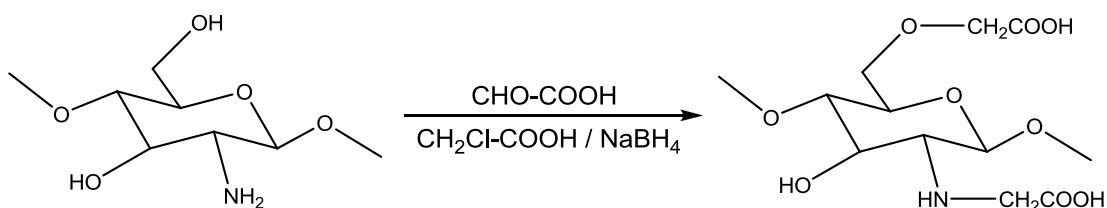
Figure 4.3 The synthesis reaction of N-O-CMC

4.4. Structural analysis of carboxymethyl chitosan

4.4.1. Infrared spectroscopy

Infrared spectroscopy is a commonly used technique to identify the chemical bonds in unknown materials. The adsorption of specific wavelength infrared light by molecules can reveal information about their molecular masses, molecular geometry and the strength of chemical bonds (Larkin, 2011). The size of absorption peaks also provides direct indications about the material amounts (Thermo Nicolet Corporation, 2001).

Diffuse reflectance infrared Fourier transform spectroscopy (DRIFTS) was used to investigate the chemical structure of the three carboxymethyl chitosan products. Measurements were conducted on a Nicolet 8700 (Thermo) instrument using a "Smart Collector" accessory. Each sample was scanned 128 times and a spectral resolution of 4 cm^{-1} was chosen. Pre-dried KBr powders (0.8 g ± 0.002 g) were thoroughly mixed and gently ground with sample powders (0.05g ± 0.002g) in an agate mortar. The mixtures were then transferred to the DRIFTS sample cell and placed in the instrument. The DRIFTS spectra were obtained with a pure KBr spectrum as the background.

4.4.2. Solid state ^{13}C nuclear magnetic resonance (NMR) spectroscopy

^{13}C NMR spectroscopy has been widely used in the structural determination of synthetic polymers (Domard et al., 1987; Cheng, 1984; Blümich et al., 1990). The chemical shifts of ^{13}C between the synthetic material and the known referential-material can provide indications of different functional groups (Dybowski et al., 2010)

Solid state ^{13}C MAS NMR measurements for chitosan and carboxymethyl chitosan were conducted on a Varian INOVA 500 MHz spectrometer at ambient temperature, using a Varian T3 HFXY 2.5 mm probe with an MAS rate of 10 kHz. The parameters for spectra acquisition were as follows: 2 s recycle delay, 200 kHz sweep width with 5 ms dwell time, and 102.4 ms for acquisition time.

4.5. Flotation tests

4.5.1. Micro-flotation

The micro-flotation tests of high purity minerals were conducted to evaluate the ability of carboxymethyl chitosan (CMC) as a selective depressant in the differential flotation of galena and chalcopyrite. A flotation tube made in-house with a Siwek et al. (1981) top, shown in Figure 4.4, was used as the flotation device. The narrow throat at the top which leads to the collection bulb only allows one bubble to pass at a time if no frother is used. This design thus minimizes mechanical entrainment. The base of the flotation tube is a

sintered glass frit with a pore size of 1.6 μm, on top of which sits a magnetic stirring bar (Cao & Liu, 2006).
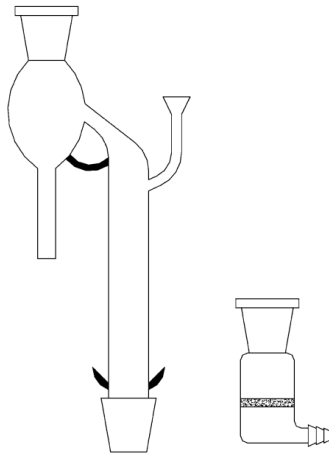
Figure 4.4 The micro-flotation device

The amount of sample (-75+45 μm) for each single mineral test or mixed mineral test (galena and chalcopyrite with a weight ratio of 1:1) was 1.5 g. The mineral samples were pre-cleaned in 0.1 mol/L hydrochloride acid solution with stirring for 5 min. After several times rinsing and filtration with distilled water, the mineral samples were suspended in 150 mL distilled water and conditioned for 2 min while the desired pH value was adjusted by hydrochloric acid or sodium hydroxide.

Purified potassium ethyl xanthate (KEX) was used as the collector, and carboxymethyl chitosan (CMC) was used as a depressant. The collector and depressant were respectively added by a desired sequence, and conditioned for 3 min after each reagent addition. The conditioned slurry was finally transferred to the flotation tube and floated for 3 min using high purity nitrogen gas. The weight recovery was calculated from the dry weights of the flotation concentrates and tails. For mixed mineral samples, the concentration of Pb and Cu in the flotation concentrate and tail were measured by a Varian SpectrAA-220FS atomic absorption spectrometer (AAS) (Varian, USA) following the desired dilution of the mixed minerals suspension which was digested with heated aqua regia.

4.5.2. Batch flotation

To investigate the selective depressant function of N-CMC in the simulation of an industrial flotation procedure, the batch flotation tests of high purity mixed minerals were conducted in a bottom-drive open top flotation cell (1.5 L, JKTech, Australia), as shown in Figure 4.5. The amount of mixed mineral sample for each test was 400 g composed of 50 g chalcopyrite, 50 g galena and 300 g quartz. In general, the batch flotation procedure consisted of two major steps: Cu-Pb bulk flotation followed by Cu-Pb differential flotation to separate chalcopyrite and galena from the bulk Cu-Pb concentrate. Detailed information about batch flotation tests can be seen in the Appendix.

(a)   (b)

Figure 4.5 JKTech flotation machine: a) side view; b) top view of 1.5 L flotation cell
         (Courtesy of Xiao Ni, 2010)

4.5.2.1. Bulk flotation

The mineral mixture sample was first wet ground with 300 mL distilled water in a rod mill (Titan Process Equipment Ltd, 17 L steel cylinder with 17 kg steel rod: $\Phi31$ mm $\times$ 2, $\Phi25$ mm $\times$ 4, $\Phi19$ mm $\times$ 8, $\Phi12$ mm $\times$ 11) for 30 seconds. Then, the slurry was transferred into

the flotation cell with constant stirring (900 rpm) and conditioned for 2 min while the pH value was adjusted to 10 by 0.5 mol/L sodium hydroxide solution. After 3 min conditioning with the desired amount of KEX, the bulk flotation was carried out for 2 min at an air flow rate of 7 L/min.

4.5.2.2. Cu-Pb separation

The bulk Cu-Pb concentrate was filled into the 1.5 L flotation cell with constant stirring (900 rpm) and conditioned while the desired pH was adjusted by hydrochloric acid or sodium hydroxide. The N-CMC and KEX were respectively added according to a desired sequence and dosage, and conditioned for 3 min after each reagent addition. Then, the differential flotation was carried out under a desired pH for 2 min at an air flow rate of 7 L/min. The weight recovery was calculated from the dry weights of the flotation concentrates and tails. The concentrations of Pb, Cu and Si in the flotation concentrate and tail were determined by a Varian SpectrAA-220FS atomic absorption spectrometer (AAS) (Varian, USA) following digestion with hot nitric acid.

4.6. Adsorption mechanism studies

The adsorption mechanisms between N-CMC and the tested minerals were investigated by a photometric dispersion analyzer (PDA), ToF-SIMS, zeta potential and XPS measurements to explain the flotation results and N-CMC's selectivity. In addition, the adsorption isotherm was studied by total carbon content measurements and the results are included in the Appendix.

4.6.1. Metal ion binding tests

The binding ability of N-CMC with copper and lead ions was investigated by a photometric dispersion analyzer (PDA 2000, Rank Brothers). The metal ion solutions were prepared individually with the same ion concentration at 0.1 mol/L. Twenty (20) mL of the metal ion solution was placed in a beaker, agitated and circulated through the PDA 2000 by a peristaltic pump. Under constant stirring, a 0.2 g/L N-CMC aqueous solution was gradually

added into the beaker in 0.25 mL increments every 30 seconds. The root-mean-square (RMS) output of the PDA 2000 was recorded.

4.6.2. ToF-SIMS imaging

Time-of-flight secondary ion mass spectrometry (ToF-SIMS) is one the most sensitive surface analytical techniques, with a resolution less than 1 nm, and a sensitivity of 1 ppm (Boulton et al., 2003). The elemental distribution maps can be obtained by rastering over interested areas with focused ion beam, and have been widely exploited to study the adsorption of reagents on mineral surfaces (Stowe et al., 1994; Brinen & Reich 1992). In this study, ToF-SIMS was utilized to characterize the adsorption density and map the distribution of N-CMC on galena and chalcopyrite's surfaces at their natural pH and pH 10.

ToF-SIMS measurements were performed on a ToF-SIMS IV-100 spectrometer (ION-TOF GmbH) with 25 keV Bi^+ primary ions. The imaging of selected ions (both positive and negative) were obtained from each specific area under the Burst Alignment mode and calibrated with peaks of H, C, O, S, CuS and PbS beforehand. 128 × 128 pixels were chosen in imaging acquisition.

The preparation procedures for samples used in this study were as follows: 1.5 g of pre-cleaned mixed minerals (galena and chalcopyrite with a weight ratio of 1:1) with a size of -20 μm was added into 150 mL distilled water and conditioned for 2 min at a desired pH. After adding 150 μL N-CMC solution (2 g/L), the suspension was conditioned in a shaking incubator for 60 min at 25℃. The minerals in suspension were then filtered and washed with distilled water through the filtration funnel three times. Before analysis, the mineral samples were dried and kept in a vacuum desiccator. To prevent surface oxidation and contamination, the samples were analysed within 12 h after being prepared.

4.6.3. X-ray photoelectron spectroscopy (XPS)

By irradiating the monoenergetic soft X-ray beam on a solid sample surface in high vacuum condition, X-ray photoelectron spectroscopy (XPS) can provide a quantitative surface-sensitive analysis for the sample. XPS spectra are obtained by recording the numbers of electrons ejected from the top few nm and their kinetic energy. The peak intensities on XPS

spectra are related to the amount of a certain material at the sample surface, while the peak position indicates the chemical composition (Fairley, 2009; Moulder et al., 1992)

In this study, XPS measurements were performed on six samples: unmodified chitosan, N-CMC, N-CMC adsorbed on chalcopyrite at pH 7, N-CMC adsorbed on chalcopyrite at pH 10, N-CMC adsorbed on galena at pH 7, and N-CMC adsorbed on galena at pH 10. The peak intensities and peak positions of these samples were compared to investigate the changes of N-CMC's chemical composition and amounts on mineral surfaces.

To prepare samples for XPS analysis, 1.5 mg N-CMC (750 µL of 2 g/L bulk solution) and 1.5 g of a single mineral (-20 µm chalcopyrite or galena) was added into 150 mL distilled water. After pH adjustment, the suspension was conditioned in a shaking incubator for 30 min at 25 ℃. The minerals were then filtered and washed with 100 mL distilled water, and further dried in a vacuum desiccator. XPS measurement were conducted within 12 hours after the sample preparation in order to minimize surface oxidation.

The XPS measurements were carried out on an AXIS 165 X-ray spectrometer (Kratos Analytical, USA) with a monochromatic Al-Kα source (1486.69 eV) at a power of 100W. For survey scan and high resolution scan, the analyze pass energies were 80 eV and 20 eV respectively, and their corresponding step sizes were 0.4 eV and 0.1 eV. Considering the particles size (-20 µm), the area of analysis was chosen as 400 µm × 700 µm on the sample surface. Software named CasaXPS (version 2.3.15) was used in the data processing of high resolution spectra. All the spectra were calibrated using C 1s at 284.8 eV. The spectra were resolved into individual peaks using the Shirley-type background and the Gaussian-Lorentzien shape.

4.6.4. Zeta potential measurements

Electrokinetic measurements can be utilized to study the adsorption behaviour of reagents in mineral flotation, since small changes in adsorption will bring significant modifications in electrokinetic potentials (Fuerstenau & Pradip, 2005)

In this study, the zeta potential measurements of chalcopyrite and galena were carried out using a ZetaPALS Zeta Potential Analyzer from Brookhaven Instrument. The

Smoluchowski model was adopted in the calculation of zeta potentials from the measured electrophoretic mobilities.

Each sample measurement was run for 10 times, with 20 measurement cycles per run. The final recorded zeta potential of each sample is the mean value without considering the highest and lowest runs.

The preparation procedures for samples were as follows:

1. A stock mineral suspension was first prepared by adding 0.5 g of -20 μm pre-cleaned mineral powders into 100 mL 10^{-2} M NaCl solution. The suspension was left to stand for 24 hours before using.

2. 10 mL of the stock mineral suspension was withdrawn after agitating the suspension fiercely. Then the 10 mL mineral suspension was diluted to 100 mL using 10^{-2} M NaCl solution. In the studies with N-CMC, the N-CMC solution was also prepared with the 10^{-2} M NaCl solution.

3. For each chosen pH value, the 100 mL diluted suspension was conditioned for 20 minutes. The pH value was adjusted and maintained by adding sodium hydroxide and hydrochloric acid solutions prepared by the 10^{-2} M NaCl solution.

4. After conditioning, 1.6 mL of suspension was transferred to the sample cell in which the electrodes were inserted for measurement.

4.7. Mineral surface cleaning test

In these tests, 1.5 g hydrochloric acid pre-cleaned galena sample (-75+45 μm) was suspended in a beaker with 150 mL distilled water, and 0.75 mL of 0.2 mol/L cupric sulfate solution was added with constant stirring for 5 min. The original concentration of Cu^{2+} in the suspension was 1×10^{-3} mol/L. Then, the galena sample was filtered and rinsed by alkaline water (pH 8) four times to avoid dissolution of the copper from the surface of galena. After vacuum drying for 12 hours, the galena sample was divided into two equal parts. One part was marked as "Blank" and suspended with only 150 mL distilled water. The other part was suspended in 150 mL distilled water but with the addition of 75 μL N-CMC solution (2 g/L), and labeled as "N-CMC". After 10 min stirring, the two suspensions

were filtered to collect the galena samples. The collected galena samples were separately washed with 20 mL of 0.1 mol/L hydrochloric acid and filtered. The filtrates were collected and analyzed by the Varian SpectrAA-220FS atomic absorption spectrometer (Varian, USA) to measure the concentration of Cu^{2+}.

5. Results and discussion

5.1. Structural analysis of carboxymethyl chitosan

5.1.1. Infrared spectroscopy

Figure 5.1 shows the DRIFTS-FTIR spectra of three carboxymethyl chitosans (CMC) and unmodified chitosan. As can be seen from the figure, the spectra of the CMCs were different from each other, indicating that they were three different substances. The characteristic peaks of CMC in the range of 700-1800 cm^{-1} were identified by comparing their spectra with that of chitosan.
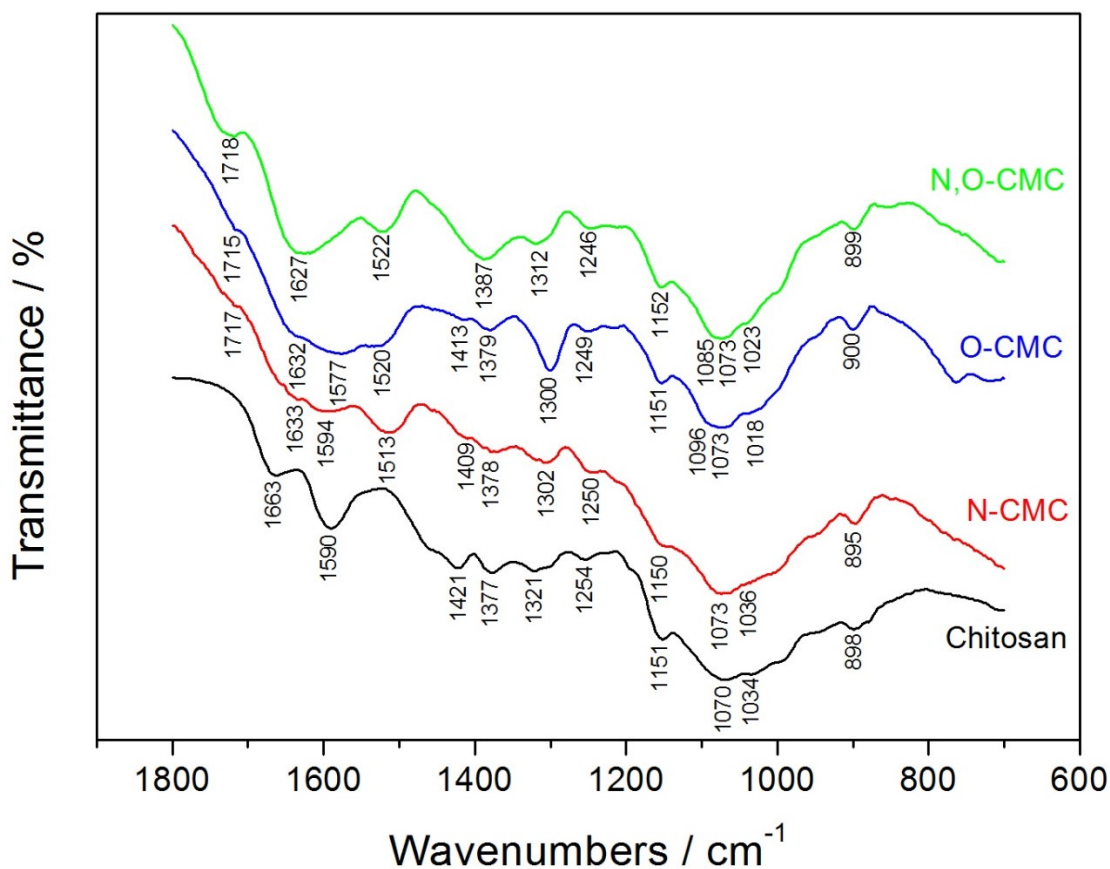
Figure 5.1 The DRIFTS spectra of unmodified chitosan and carboxymethyl chitosan

5.1.1.1. Characteristic peaks of chitosan

The spectrum of unmodified chitosan powder was analyzed based on the investigation of Pearson et al. (1960). It shows a characteristic peak of amide I at 1663 cm^{-1} (C=O stretching) with relatively low intensity due to the high DA of the chitosan sample. In the meantime, the peak of N-H deformation in the amino group at 1590 cm^{-1} (N-H deformation of –NH$_2$) has a relative strong intensity and covers up the peak of amide II at 1556 cm^{-1} (N-H deformation in amide group). The peaks at 1377 cm^{-1} and 1321 cm^{-1} are assigned as O-H deformation of –CH$_2$-OH and –CH-OH, respectively. The peaks at 1034 cm^{-1} and 1070 cm^{-1} belong to the C-O stretching of –CH$_2$-OH and –CH-OH, respectively. The peak at 1151 cm^{-1} comes from the asymmetric stretching of the bridge oxygen (C-O-C).

5.1.1.2. Characteristic peaks of N-CMC

In the spectrum of N-CMC, the newly appeared peaks at 1717 cm^{-1} and 1302 cm^{-1} can be assigned to the C=O stretching and C-O stretching of –COOH, respectively (Sahu et al., 2011; Larkin, 2011), which illustrate the successful introduction of the carboxymethyl group. Another new peak at 1513 cm^{-1} also appeared, in comparison with a dramatic decrease in the intensity of the peak at 1594 cm^{-1}. This phenomenon indicates that the amino groups were the main substitution sites for N-CMC, and the peak at 1513 cm^{-1} can be assigned as N-H deformation of –NH– (Larkin, 2011). As a consequence of incomplete substitution, the peak of N-H deformation (–NH$_2$) at 1594 cm^{-1} (Larkin, 2011; Chen & Park, 2003) can still be observed but with a lower intensity. Due to the substitution on the amino groups, the C-N stretching of –C-NH$_2$ at 1421 cm^{-1} also shifts to 1409 cm^{-1} (Mourya et al., 2010; Pearson et al., 1960). The characteristic peaks of the –CH$_2$-OH at 1378 cm^{-1} and 1036 cm^{-1}, and peaks of –CH-OH at 1318 cm^{-1} (overlapped by the peak at 1302 cm^{-1}) and 1073 cm^{-1}, do not show any shift or change compared to the original peaks on chitosan. Their shifts are within the resolution of the infrared spectrometer which indicates that hydroxyl groups are likely not involved in the substitution.

5.1.1.3. Characteristic peaks of O-CMC

Similarly, the peaks at 1715 cm^{-1} and 1300 cm^{-1} on O-CMC's spectrum belong to the C=O stretching and C-O stretching of –COOH respectively, indicating that the carboxymethyl

group has been introduced on O-CMC. During O-CMC's synthesis, the addition of 1% hydrochloric acid resulted in the ionization of -NH_2 into –NH_3^+. Therefore, the peak at 1590 cm^{-1} (N-H deformation of –NH_2) on chitosan shifts to 1577 cm^{-1} (N-H deformation of –NH_3^+) on O-CMC's spectrum (Chen & Park, 2003; Mourya, Inamdar & Tiwari, 2010). The new peak at 1520 cm^{-1} with a low intensity can be assigned to the symmetric –NH_3^+ deformation vibration (Huang, Cao & Liu, 2012b; Muzzarelli et al., 1982). The shift of C-N stretching from 1421 cm^{-1} to 1413 cm^{-1} is also due to the ionization. Another new peak at 1096 cm^{-1}, corresponding to the C-O-C asymmetric stretching of –CH_2-O-CH_2–, shows that the primary hydroxyl groups were the substitution sites for O-CMC (Larkin, 2011; Chen & Park, 2003).

5.1.1.4 Characteristic peaks of N-O-CMC

Similar to the other two CMC products, the peaks of –COOH at 1718 cm^{-1} and 1312 cm^{-1} appeared in N-O-CMC's spectrum with strong intensities. Both the peak of –NH– at 1522 cm^{-1} (overlapped with symmetric –NH_3^+ deformation) and the peak of –CH_2-O-CH_2– at 1085 cm^{-1} can be observed on N-O-CMC. Their coexistence illustrates that the amino groups and the primary hydroxyl group both took part in the substitution reaction.

5.1.2. Solid state ^{13}C nuclear magnetic resonance (NMR) spectroscopy

Figure 5.2 shows the solid-state ^{13}C NMR spectra of the three synthesized CMC products and the spectrum of unmodified chitosan. Figure 5.3 shows the structure of chitosan, indicating where the C_1, C_2, C_3, C_4, C_5 and C_6 locate.

According to previous studies (Wang & Liu, 2013; Rinaudo et al., 1992), C_1, C_2, C_3, C_4, C_5 and C_6 on the spectrum of chitosan are identified as peaks at 105.3 ppm, 57.6 ppm, 61.3 ppm, 72.6 ppm, 75.4 ppm and 82.7 ppm, respectively. It can be seen from the spectra of CMC that, C_2 and C_6 peaks on the CMC products have the most apparent changes and shifts. This phenomenon indicates that either C_2, C_6 or both provided the substitution sites for the carboxymethyl groups in CMC. To locate the exact substitution site, the ^{13}C NMR spectra were resolved to focus on the peaks of C_2 and C_6.
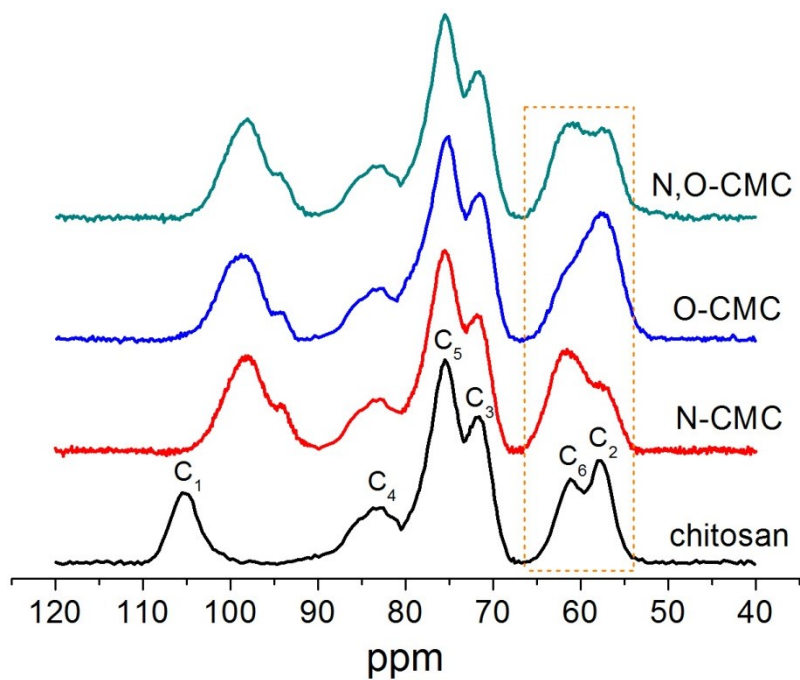
Figure 5.2 Solid-state ^{13}C NMR spectra of chitosan and the three carboxymethyl chitosans
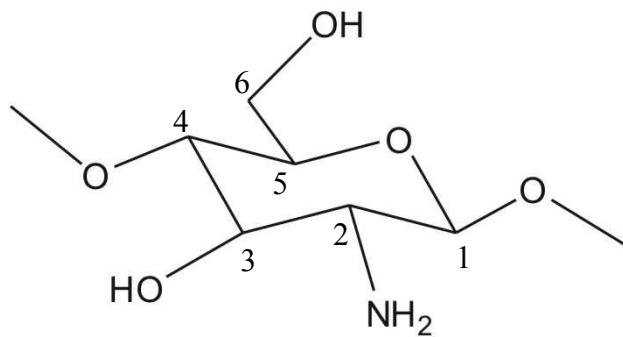
Figure 5.3 The structure of chitosan with the positions of carbon marked (Tiwary et al., 2011)
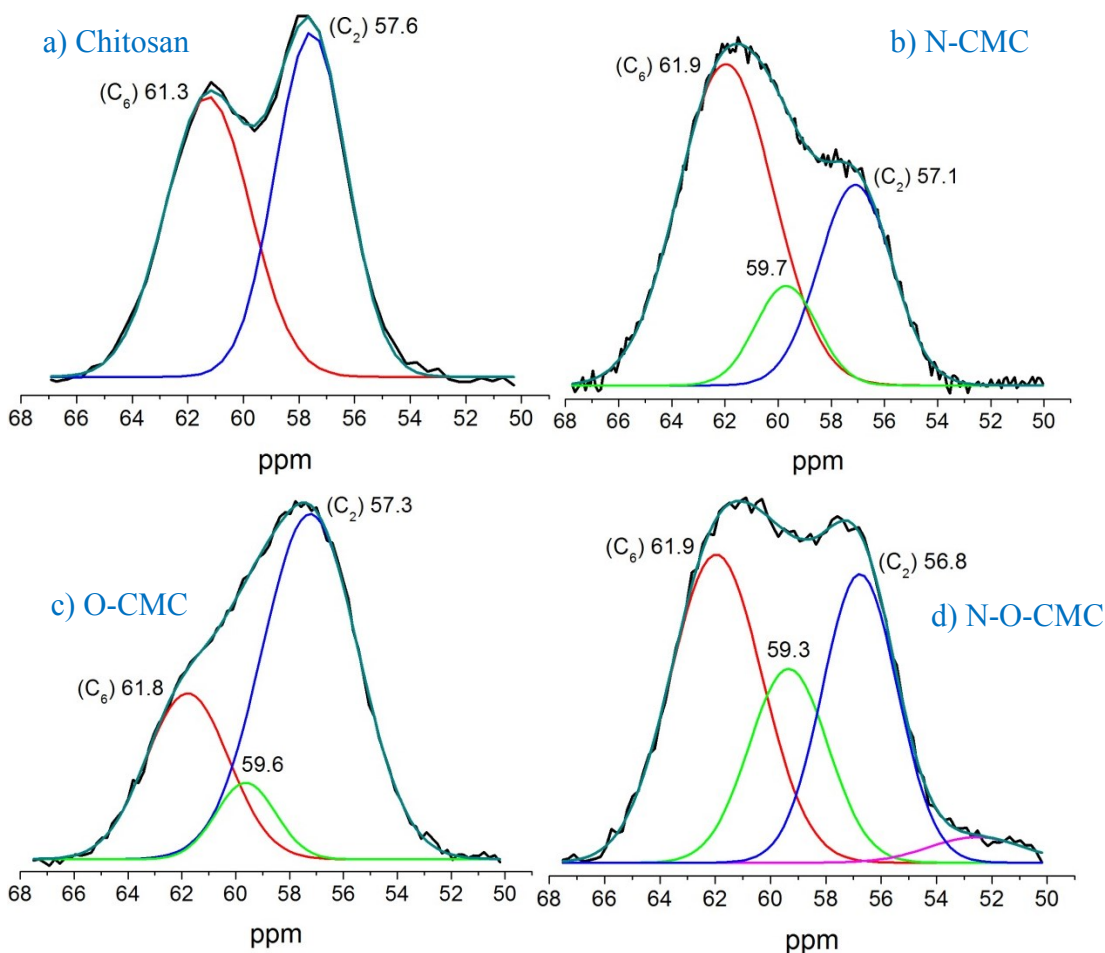
Figure 5.4 The resolved solid-state ^{13}C NMR spectra of: a) chitosan, b) N-CMC, c) O-CMC, and d) N-O-CMC.

The resolved NMR spectra of CMC and chitosan with only C_2 and C_6 peaks are shown in Figure 5.4. For chitosan, the original peaks of C_2 (C-NH$_2$, amino group) and C_6 (C-OH, primary hydroxyl group) can be observed at 57.6 ppm and 61.3 ppm respectively.

For N-CMC, in comparison with chitosan, the intensity of C_2 decreases significantly. In addition, the peak of C_2 shifts to a higher ppm value. By adding more glyoxylic acid (CHO-COOH) in the synthesis process, the peak intensity of C_2 becomes even lower, as shown in Figure 5.5. Therefore, the substitution indeed happened on the amino group (C_2).
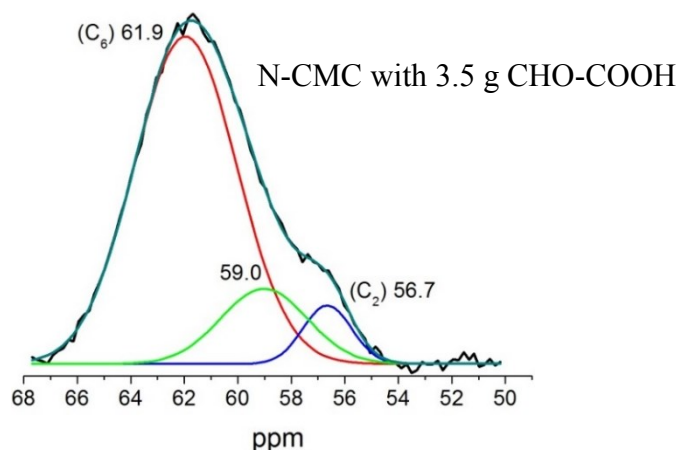
Figure 5.5 The resolved solid-state ^{13}C NMR spectra of N-CMC with 3.5 g CHO-COOH.

For O-CMC, the intensity of C_6 becomes lower when compared with the peaks on chitosan. Meanwhile, partial C_6 shifts to lower ppm value, slightly broadens the peak of C_2. These changes show that the primary substitution site is the hydroxyl group on C_6.

For N-O-CMC, the peaks of C_2 and C_6 both have lower intensities compared with the original peaks on chitosan. It can be possibly attributed to the shifts of two peaks: the downward shift of C_6 and the upward shift of C_2, whose overlap creates more peak area. Since both peaks shift on N-O-CMC, it can be assumed that both the amino group (C_2) and the primary hydroxyl group (C_6) provided the sites for substitution.

5.1.3. Summary

According to the results from infrared spectroscopy and NMR analyses, the structures of the three carboxymethyl chitosan products can be confirmed as follows:
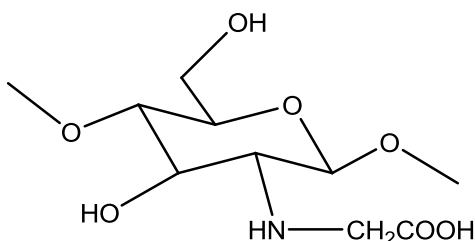
Figure 5.6 N-CMC structure

In N-CMC, only the amino groups were substituted by carboxymethyl groups and its structure is shown as Figure 5.6.
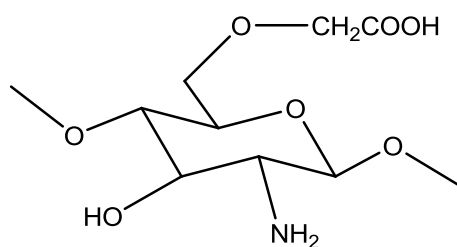
Figure 5.7 O-CMC structure

For O-CMC, only the primary hydroxyl groups on C_6 were replaced by carboxymethyl groups and its structure is illustrated as Figure 5.7.
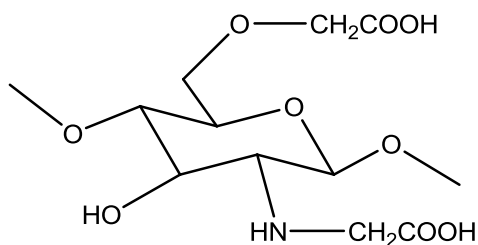
Figure 5.8 N-O-CMC structure

For N-O-CMC, both the amino groups and the primary hydroxyl groups on C_6 were substituted by carboxymethyl groups and its structure can be drawn as Figure 5.8.

5.2. Flotation tests

5.2.1. Single mineral micro-flotation
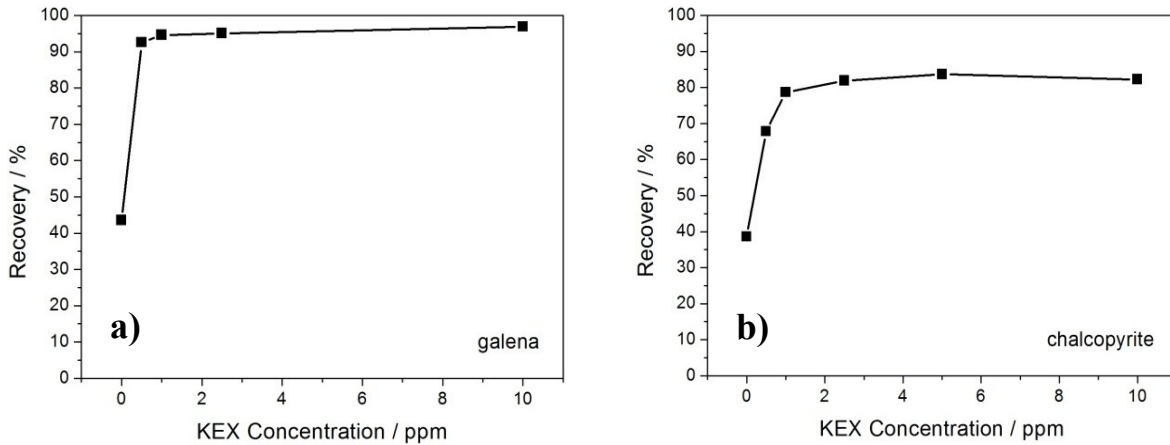
Figure 5.9 The recovery of single mineral micro-flotation as a function of KEX concentration at natural pH (6.8-7.0). 1.5 g mineral, 150 mL distilled water. Flotation time: 3 min. (a) The recovery of galena. (b) The recovery of chalcopyrite.

The critical concentration of KEX in micro-flotation was determined before any depressants were added. As shown on Figure 5.9, when KEX concentration reaches 2.5 ppm, the recoveries for both galena and chalcopyrite reach their maximum values. Therefore, the critical concentration of KEX in micro-flotation can be set as 2.5 ppm. Due to the poor solubility, O-CMC has been ruled out as a depressant. Only N-CMC and N-O-CMC were used in the following micro-flotation tests.

5.2.1.1. Single mineral micro-flotation using N-CMC as the depressant

Under natural pH (6.8-7) and the fixed collector concentration of 2.5 ppm, N-CMC was added to observe its depressant effect on the two sulfide mineral samples respectively (reagent adding sequence was N-CMC followed by KEX). Figure 5.10a shows that chalcopyrite was apparently depressed, as its recovery sharply dropped from 85% to 5% at 1 ppm N-CMC, and then remained at around 5% at higher N-CMC concentrations. However, the recovery of galena was not affected and remained around 95% in the entire N-CMC concentration range tested (up to 10 ppm).
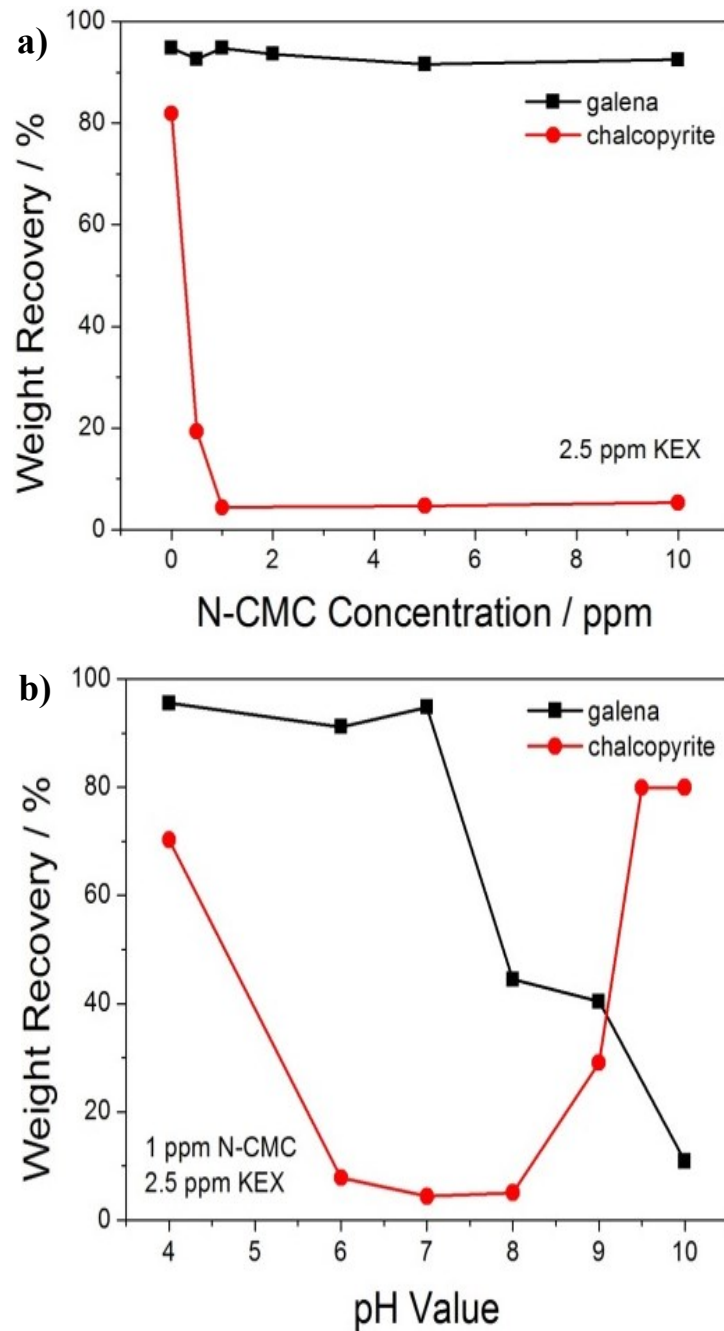
Figure 5.10 Single mineral micro-flotation of galena and chalcopyrite using N-CMC as a depressant and KEX as a collector. 1.5 g mineral, 150 mL distilled water, 2.5 ppm KEX. Flotation time: 3 min. (a) With different concentration of N-CMC at natural pH (6.8-7). (b) At different pH with 1 ppm N-CMC.

The flotation behavior of chalcopyrite and galena was then tested individually at different pH at a fixed N-CMC concentration of 1 ppm. As can be seen in Figure 5.10b, the recovery

of galena did not change too much and remained at around 95% in the slightly acidic and neutral solution, but dramatically decreased at higher pH and dropped to 10% at pH 10. Interestingly, the recovery of chalcopyrite showed a "U" shape with the lowest recovery (about 5%) occurring between pH 6 and 8. At the acidic and alkaline pH, the recovery of chalcopyrite was above 70%. Obviously, two separation windows exist: One is at pH 7, where chalcopyrite can be depressed by N-CMC but galena can be floated; another is expected to be above pH 10, where galena is depressed by N-CMC and chalcopyrite can be floated.

5.2.1.2. Single mineral micro-flotation N-O-CMC as the depressant

When pH remained under natural value (6.8-7) and the collector concentration was fixed at 2.5 ppm, different concentrations of N-O-CMC were added in several single mineral micro-flotation tests to investigate its depressing effect (reagent adding sequence was N-O-CMC followed by KEX). As shown in Figure 5.11a, by increasing the concentration of N-O-CMC, both galena and chalcopyrite tended to have lower recoveries. Chalcopyrite was completely depressed with only 3 ppm N-O-CMC, whereas at least 10 ppm N-O-CMC was required to depress galena.
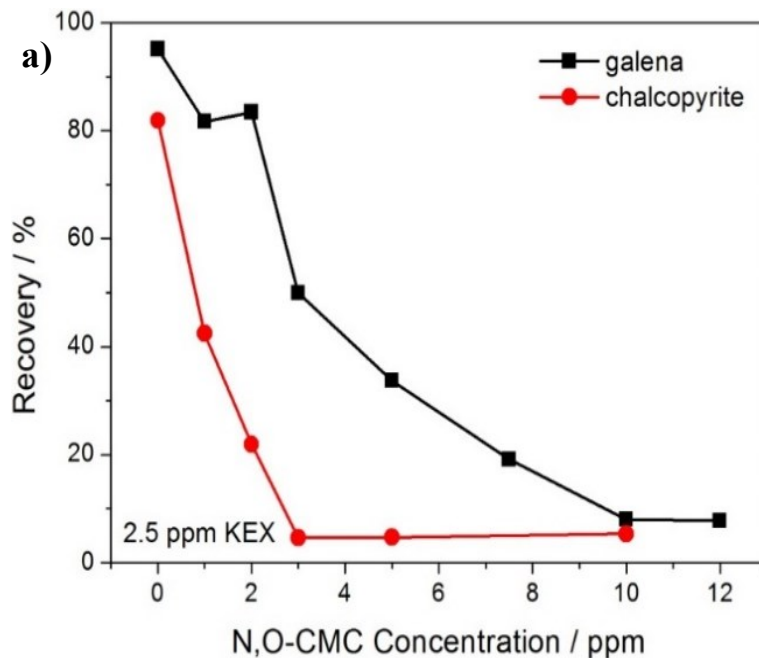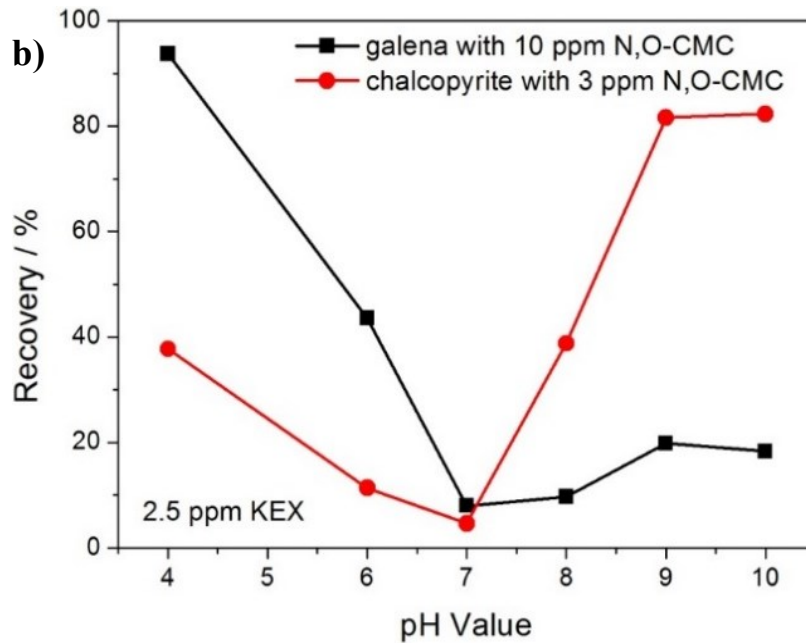
Figure 5.11 Single mineral micro-flotation of galena and chalcopyrite using N-O-CMC as a depressant and KEX as a collector. 1.5 g mineral, 150 mL distilled water, 2.5 ppm KEX. Flotation time: 3 min. (a) With different concentration of N-O-CMC at natural pH (6.8-7). (b) At different pH with 10ppm N-O-CMC for galena and 3 ppm N-O-CMC for chalcopyrite.

The flotation behaviour of galena and chalcopyrite at different pH was then investigated independently with the critical concentrations of KEX and N-O-CMC (2.5 ppm KEX; 10 ppm N-O-CMC for galena, 3 ppm N-O-CMC for chalcopyrite). As can be seen from Figure 5.11b, the recovery of galena decreased sharply from the acidic to neutral pH condition and dropped to about 8% at pH 7. This was followed by a slight increase in the recovery at higher pH, remaining at about 20% at pH 9-10. It indicates that N-O-CMC had a good depressing effect on galena under neural and alkaline pH condition. For chalcopyrite, the recovery again was the lowest at the neutral pH resembling N-CMC. The recovery was about 5% at pH 7, around 40% under acidic pH and above 80% at pH over 9. Therefore, the depressive effect of N-O-CMC on chalcopyrite was weaker under acidic and alkaline pH. Since acidic pH is not ideal for sulfide ore flotation, only one separation window may be used when using N-O-CMC as a depressant: at pH 10, galena can be depressed by N-O-CMC while chalcopyrite is floated.

5.2.2. Mixed minerals micro-flotation

5.2.2.1. Mixed minerals micro-flotation using N-CMC as the depressant

As discussed previously in the single mineral micro-flotation tests of chalcopyrite and galena, when N-CMC is used as the depressant, the separation of the two sulfide minerals can be expected at natural pH (6.8-7) or at pH 10. Based on these results, the differential micro-flotation tests on mixed minerals (chalcopyrite and galena with 1:1 weight ratio) were carried out to verify the selectivity of N-CMC. The results are shown in Figure 5.12, in which the yield represents the total weight of concentrates collected from each flotation (normalized to the initial feed weight), and the recovery of Cu or Pb was calculated from Cu or Pb assay data for the flotation concentrate and tail.

With the same reagent addition sequence (N-CMC followed by KEX) and dosage (1 ppm N-CMC and 2.5 ppm KEX), N-CMC exhibited different depressant functions at different pH, similar to single mineral flotation. Figures 5.12a shows that at pH 6.8, the concentrate yield was about 51%, which recovered 84% of the Pb but only 15% of the Cu. At pH 10, the concentrate yield was 63% and it recovered 88% of the Cu, but only 41% of the Pb. Therefore, at neutral pH, most of the chalcopyrite was depressed by N-CMC while most of the galena was floated, and the gap between galena recovery and chalcopyrite recovery was about 70 percentage points. Although under alkaline conditions galena was indeed depressed, the gap between chalcopyrite recovery and galena recovery was barely about 50 percentage points, which was not considered sufficient to separate them well.
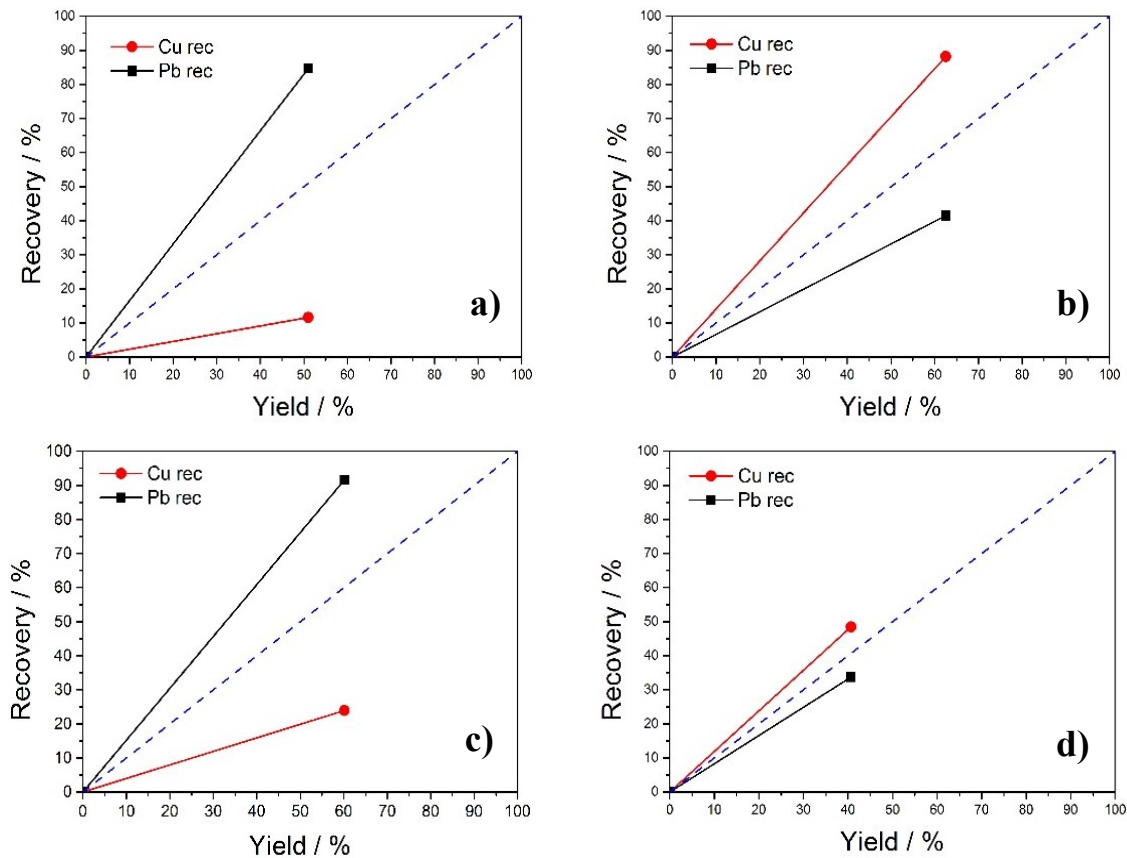
Figure 5.12 Mixed minerals micro-flotation of galena and chalcopyrite (weight ratio 1:1) using N-CMC as a depressant and KEX as a collector. 1.5 g mineral, 150 mL distilled water. Flotation time: 3 min. (a) 1 ppm N-CMC followed by 2.5 ppm KEX, pH 6.8; (b) 1 ppm N-CMC followed by 2.5 ppm KEX, pH 10; (c) 2.5 ppm KEX followed by 5 ppm N-CMC, pH 6.8; (d) 2.5 ppm KEX followed by 5 ppm N-CMC, pH 10.

As shown in Figures 5.12c and d, the dosages of N-CMC and KEX were increased to 5 ppm and 2.5 ppm, respectively. In addition, KEX was added prior to N-CMC. As can be seen, at neutral pH (Figure 5.12c), chalcopyrite was still selectively depressed by N-CMC while galena was floated. The concentrate yield was 60% which recovered 92% of the Pb and 24% of the Cu. However, at pH 10, the yield of concentrate was 41% and it recovered 48% of the Cu and 34% of the Pb. The selective depressing ability of N-CMC did not seem to exist at pH 10 and the higher reagent dosages.

5.2.2.2. Mixed minerals micro-flotation using N-O-CMC as the depressant

Since N-O-CMC only showed its selectivity at pH 10 in single mineral micro-flotation tests, a trial micro-flotation test for mixed minerals (chalcopyrite and galena with 1:1 weight ratio) with N-O-CMC was conducted at pH 10 to investigate its ability in separating the two sulfide minerals. As shown in Figure 5.13, the concentrate yield was 72% which recovered 91% of the Cu and 58% of the Pb. Therefore, even at the high dosage of 10 ppm, the N-O-CMC did not depress chalcopyrite and only slightly depressed galena, and the selectivity was very weak. It can be seen that N-O-CMC's application as a selective depressant in sulfide minerals is not very promising compared with N-CMC.
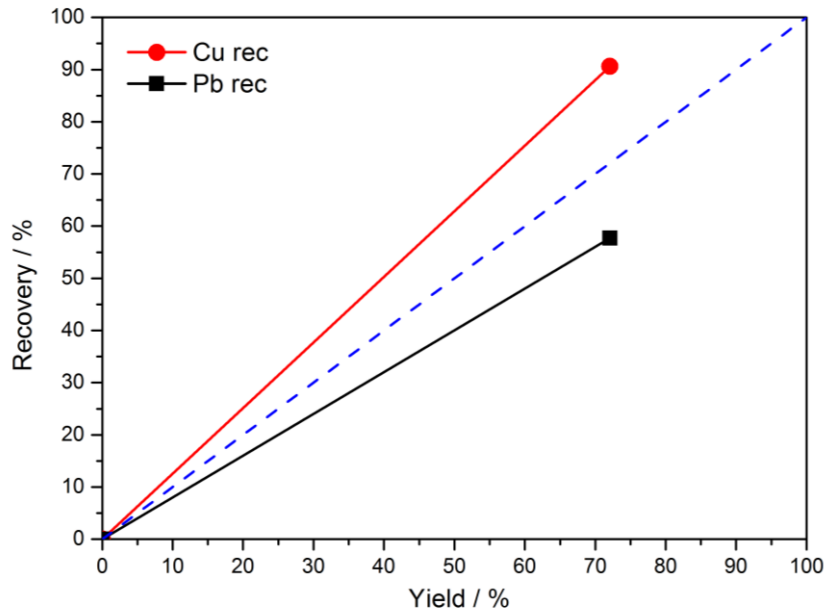
Figure 5.13 Mixed minerals micro-flotation of galena and chalcopyrite (weight ratio 1:1) using N-O-CMC as a depressant and KEX as a collector. 1.5 g mineral, 150 mL distilled water. Flotation time: 3 min. 2.5 ppm KEX followed by 10 ppm N-O-CMC, pH 10.

5.2.3. Batch flotation

Due to the poor selectivity and depressing effect of N-O-CMC in mixed minerals micro-flotation tests, only N-CMC was further studied in batch flotation tests. The batch flotation tests were conducted to investigate the selective depressant function of N-CMC in the simulation of an industrial flotation procedure, i.e., a Cu-Pb bulk flotation followed by Cu-Pb separation. Figure 5.14 shows the results of one of these batch flotation tests. In this figure, the yield is the weight of the flotation concentrate normalized against the weight of the Cu-Pb bulk concentrate. As can be seen, at 58% yield, the flotation concentrate recovered 89% of the Pb and 24% of the Cu. The selective depressant ability of N-CMC can, therefore, be expected in industrial applications.
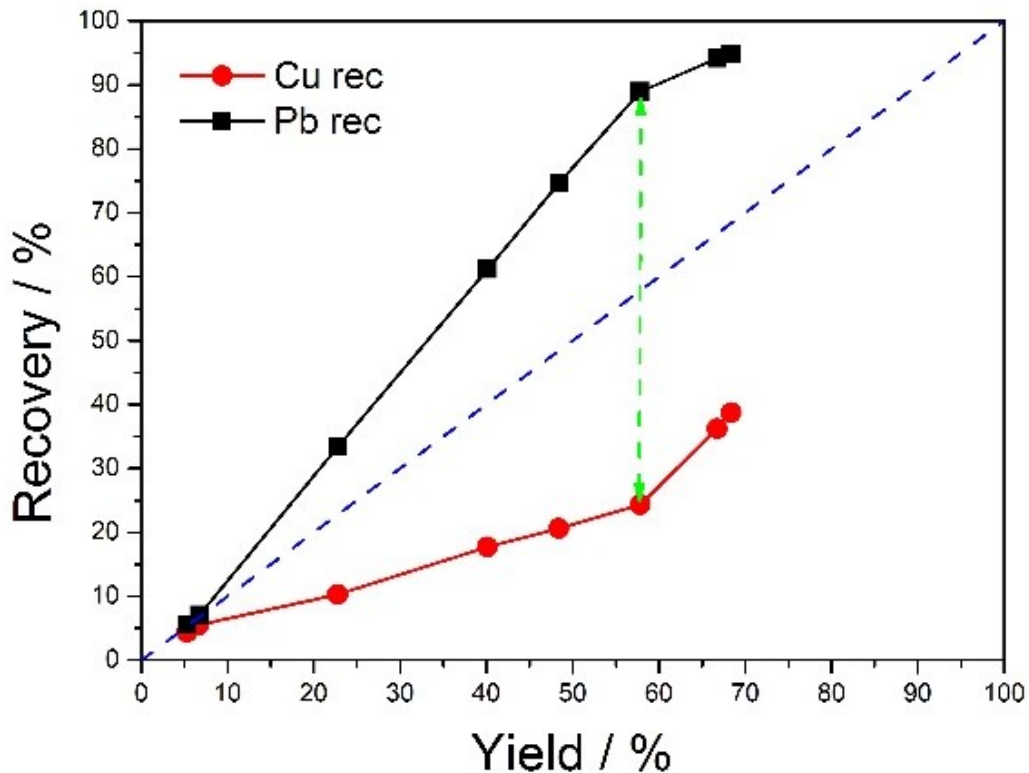
Figure 5.14 Batch flotation for mixed minerals of galena and chalcopyrite

5.2.4 Summary

During the single mineral micro-flotation tests, two separation windows are observed for N-CMC: One at pH 7 where chalcopyrite is depressed by N-CMC but galena can be floated, and another is above pH 10 where galena is depressed by N-CMC and chalcopyrite can be floated. For N-O-CMC, galena can be depressed by N-O-CMC while chalcopyrite can be floated at pH 10.

Based on mixed mineral flotation results, the addition sequence of collector (KEX) and depressant (CMC) will not affect the selectivity of the depressant. For N-CMC, at neutral pH, most of the chalcopyrite was still depressed by N-CMC while most of the galena was floated, and the difference between their recoveries can be as high as 70 percentage points. While at pH 10, N-CMC's selectivity became weak and the separation of two minerals became difficult. When using N-O-CMC as a depressant in mixed mineral flotation, both galena and chalcopyrite were floated and the selectivity was absent.

N-CMC was used in batch flotation tests which simulated commercial bulk Cu-Pb flotation followed by Cu-Pb differential flotation. The results indicated that Cu-Pb separation was achieved by depressing chalcopyrite while floating galena.

The reason for N-CMC's selectivity will be discussed in the next section via its adsorption mechanism onto galena and chalcopyrite surfaces.

5.3. Adsorption mechanism studies

5.3.1. Metal ions binding tests

Photometric dispersion analysis was performed to gain an understanding of the binding capacity of N-CMC with metal ions. The PDA 2000 photometric dispersion analyzer monitors the in-situ precipitation process of N-CMC at different dosages with Cu^{2+} and Pb^{2+} ions. When the metal ions react with N-CMC, the initially clear metal ion and N-CMC solutions would turn cloudy to show the formation of precipitates. The particle size of the precipitates was represented by the "RMS" signal (root mean square value of the amplified ac signal) of the PDA 2000 photometric dispersion analyzer, since the appearance and/or

flocculation of particles can cause a great increase of the RMS readings (Rank Brothers Ltd, 2013).

As can be seen from Figure 5.15, the RMS output of the PDA 2000 continuously increased when N-CMC was gradually added to a cupric sulfate solution. However, the RMS output maintained a stable low value when N-CMC was added to a lead nitrate solution. It, therefore, seems that N-CMC had a stronger binding capacity with Cu^{2+} than with Pb^{2+}. It can also be assumed that the different depressing effect of N-CMC on chalcopyrite and galena possibly originates from its different affinities to the lattice metal ions in these minerals.
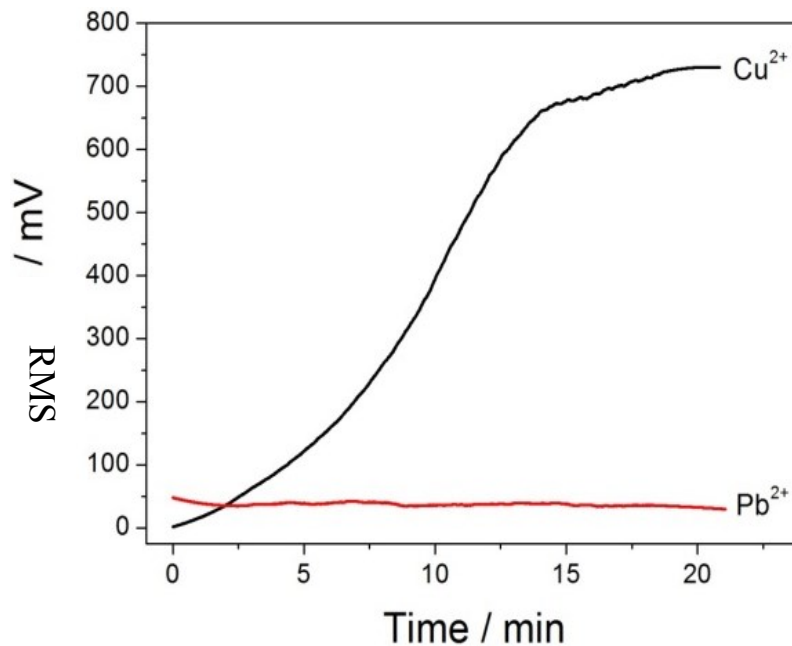
Figure 5.15 Photometric dispersion analyzer root-mean-square output of Cu^{2+} and Pb^{2+} binding with N-CMC. 20 mL cupric sulfate or lead nitrate solution (0.1 mol/L) was titrated with a 0.2 g/L N-CMC solution in 0.25 mL increment every 30 seconds.

5.3.2. ToF-SIMS imaging

Both negative and positive ion spectra were generated for mineral samples at natural pH and pH 10. Two representative spectra were selected to illustrate the adsorption of N-CMC on galena and chalcopyrite. COOH was used to indicate the carboxyl group on N-CMC. NH_2 came from the unmodified monomers of chitosan without carboxylmethyl groups. $C_2H_4NO_2$, as the carboxymethyl group grafted on N, was used to delineate the distribution of N-CMC. CuS and PbS represented chalcopyrite and galena, respectively. The position of each ion was shown on the map in bright colours.
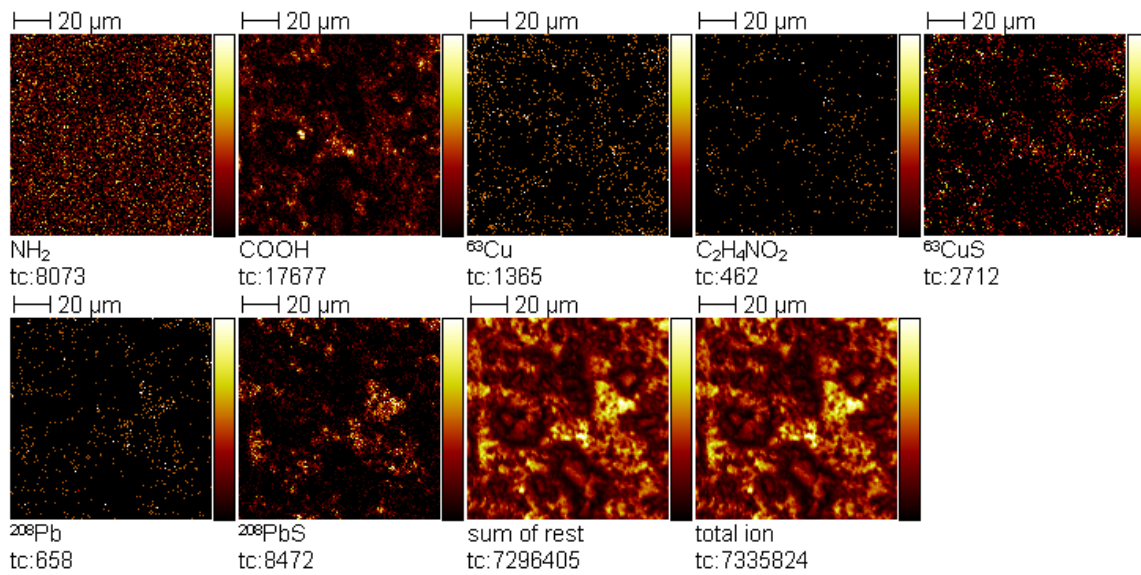
Figure 5.16 Negative ion spectra at natural pH (107 μm ×107 μm)

Figure 5.16 shows the negative ion spectra at the natural pH condition on an area of 107 μm ×107 μm. As can be seen, images of COOH and $C_2H_4NO_2$ match the pattern of CuS. Both COOH and $C_2H_4NO_2$ were from the N-CMC, indicating that N-CMC adsorbed mostly on the chalcopyrite. This result is in accordance with the flotation tests, in that N-CMC depressed chalcopyrite at natural pH. It can also be seen that at natural pH, carboxyl groups played an important role in the selectivity of N-CMC. However, the distribution of N-CMC still has some overlap area with galena, as can be seen from the images of COOH and PbS. This phenomenon is also supported by mixed mineral flotation results that about 20% galena was depressed by N-CMC at natural pH. The positions of NH_2 seem to be evenly distributed on the image, and do not show any preference towards either sulfide

mineral. Therefore, the NH$_2$ groups seem to have no impact on N-CMC's selectivity at natural pH.
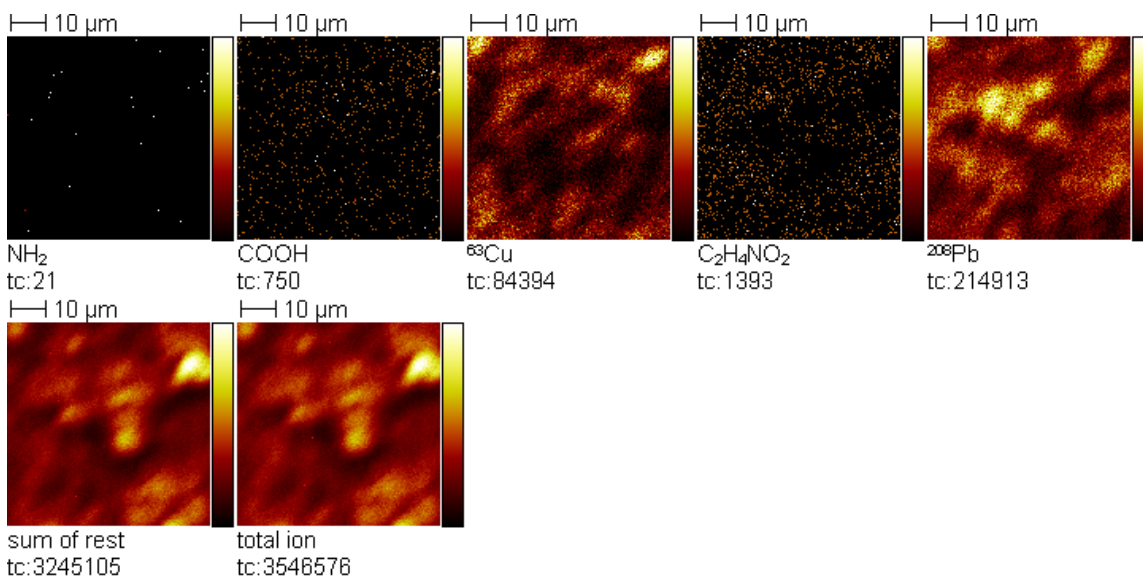
Figure 5.17 Positive ion spectra at pH 10 (55.7 μm × 55.7 μm)

Figure 5.17 shows the positive ion spectra at pH 10 on a region of 55.7 μm × 55.7 μm. The images of Cu and Pb complement each other very well, but the distributions of COOH and C$_2$H$_4$NO$_2$ show no obvious resemblance with either Cu or Pb. It seems that there was no preference of N-CMC's adsorption on either mineral particles. It is consistent with the mixed minerals micro-flotation tests at pH 10.

5.3.3. X-ray photoelectron spectroscopy (XPS)

XPS was utilized to investigate the adsorption bonds formed between N-CMC and mineral. The XPS survey scan and narrow scan of N 1s were first conducted on unmodified chitosan and N-CMC. The XPS spectra of N 1s were also collected on chalcopyrite and galena after they were treated by N-CMC at either pH 6.8 or at pH 10. By comparing the N 1s binding energies, a better understanding of the adsorption process can be obtained.

5.3.3.1. The N 1s spectrum of chitosan
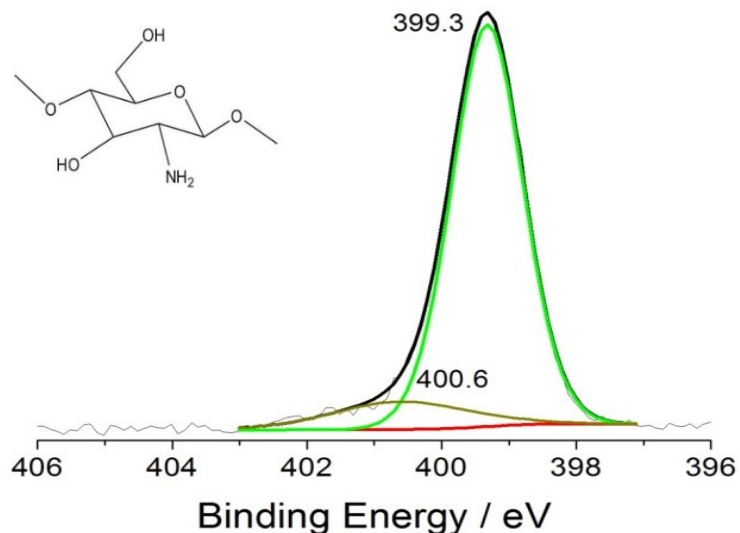
Figure 5.18 The resolved narrow scan N 1s spectrum of chitosan

As shown in Figure 5.18, two peaks can be resolved on the narrow scan N 1s spectrum of chitosan. The peak at 399.3 eV is assigned to –NH$_2$ (the basic structural unit of chitosan). Another peak at 400.6 with a small intensity belongs to O=C–NH– (amide in acetyl group), which is the undeacetylated part of chitosan.

5.3.3.2. The N 1s spectrum of N-CMC
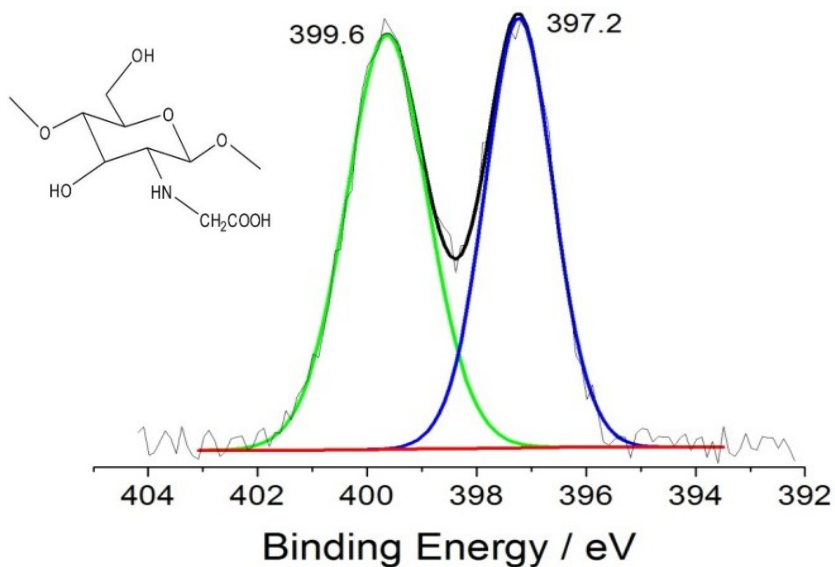
Figure 5.19 The resolved narrow scan N 1s spectrum of N-CMC

Compared to the spectrum of chitosan, the binding energy of N 1s on N-CMC has significant changes after the carboxymethylation, as shown in Figure 5.19. Since one hydrogen of $-NH_2$ on chitosan has been replaced by the carboxymethyl group, $-NH_2$ changes to $-NH-$. The peak at 399.6 eV on CMC is due to the shift of the peak at 399.3 eV on chitosan, and the shifted peak can be assigned as $-NH-$. Meanwhile, a new peak appears at 397.2 eV on the N 1s spectrum of N-CMC with a high intensity. According to the NIST XPS database version 2.0 (Wagner et al., 1997), this peak can be attributed to $-NH-CH_2-COOH$. The peak at 400.6 eV on chitosan is probably overlapped with the upward shifted peak of $-NH-$.

5.3.3.3. The N 1s spectrum of N-CMC treated chalcopyrite at pH 7
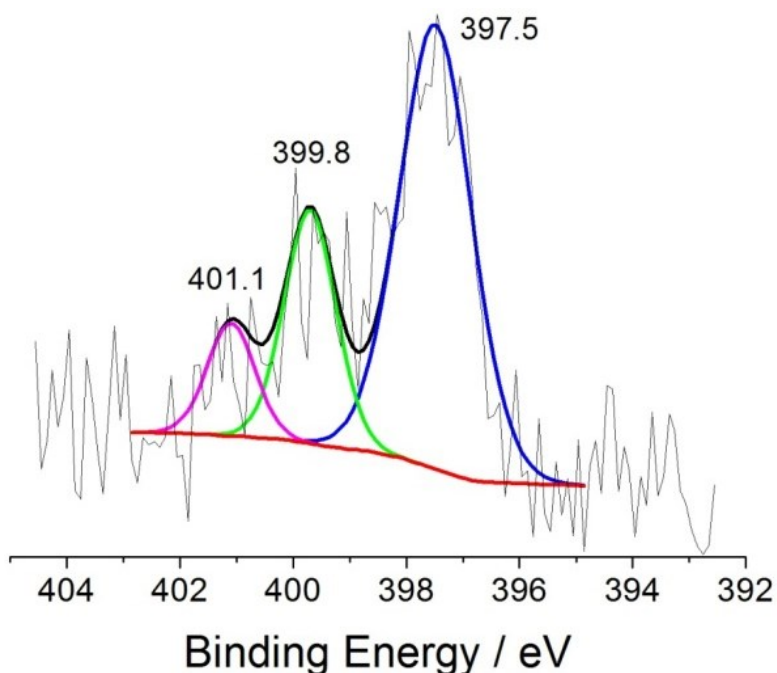
Figure 5.20 The resolved narrow scan N 1s spectrum of N-CMC on chalcopyrite at pH 7

As can be seen from Figure 5.20, the peak of $-NH-$ and the peak of $-NH-CH_2-COOH$ shift upwardly to 399.8 eV and 397.5 eV respectively, compared to the N 1s spectrum of N-CMC. The shifts of peaks can be attributed to the bonds formed between $-COOH$ and Cu. Due to this interaction, the distribution of electron cloud density will migrate to the copper side, leading to the upward shifts of the $-NH-$ peak (from 399.6 eV to 399.8 eV) and the $-NH-CH_2-COOH$ peak (from 397.2 eV to 397.5 eV). In addition, a new peak appeared at

401.1 eV, most likely due to the direct bonds formed between Cu and N on secondary amino groups.

5.3.3.4. The N 1s spectrum of N-CMC treated chalcopyrite at pH 10
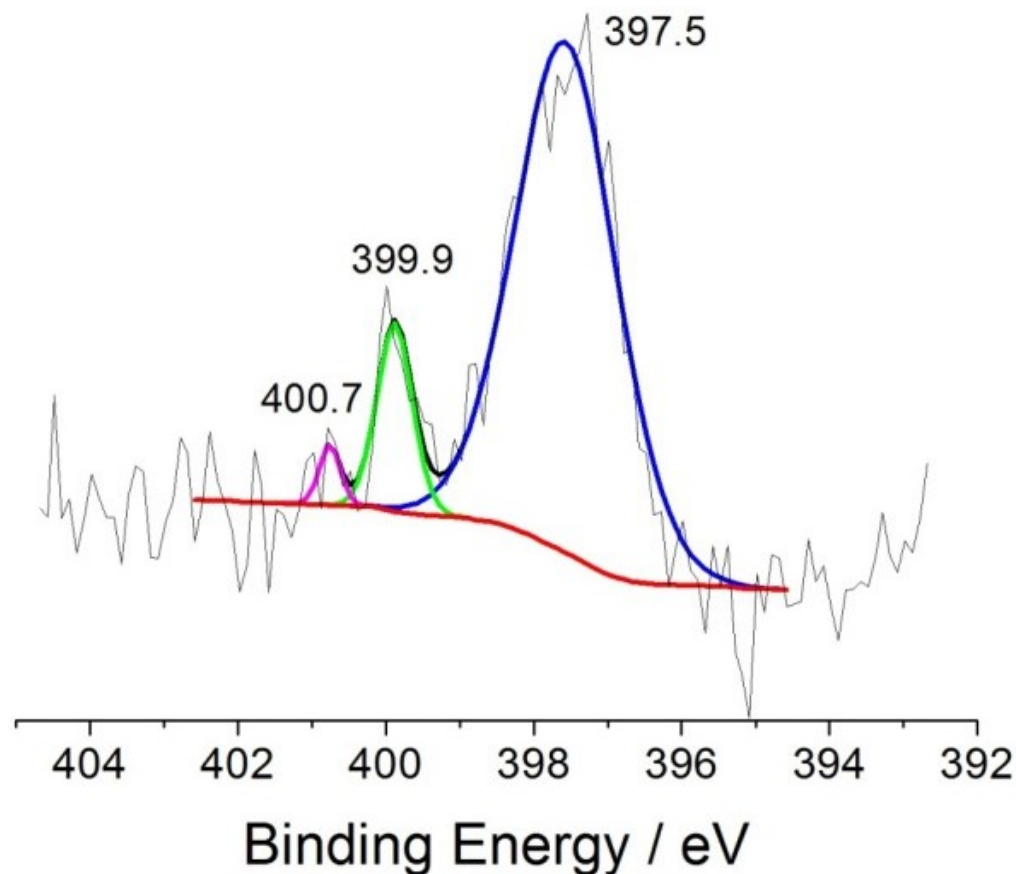
Figure 5.21 The resolved narrow scan N 1s spectrum of N-CMC on chalcopyrite at pH 10

Figure 5.21 shows that similar peak shifts were observed at pH 10. The peak of –NH– now shifts to 399.9 eV while the peak of –NH-CH_2-COOH shifts to 397.5 eV, as a result of the interaction between Cu and –COOH. A new peak appears at 400.7 eV with a low intensity, indicating that a very weak bond formed between Cu and the secondary amino group. It also implies that only a limited amount of secondary amino groups are involved in the binding reaction.

5.3.3.5. The N 1s spectrum of N-CMC treated galena at pH 7
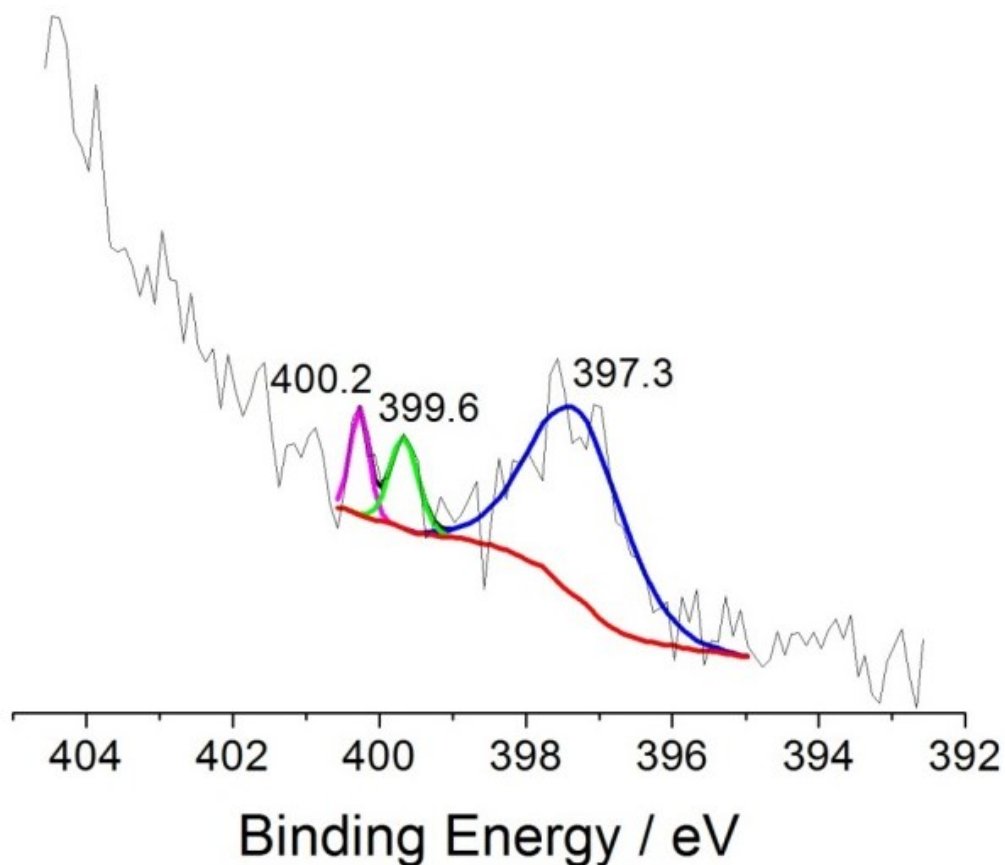
Figure 5.22 The resolved narrow scan N 1s spectrum of N-CMC on galena at pH 7

Compared with N-CMC's spectrum (Figure 5.19), after the adsorption on galena at pH 7, the peak of –NH-CH2-COOH only changed by 0.1 eV which is within the resolution of the XPS measurement (Figure 5.22). Meanwhile, the peak of –NH– did not shift. Therefore, there seems to be no direct bonding between Pb and –COOH. When compared to the N 1s spectrum on galena at pH 10 (Figure 5.23), the average peak intensity on galena at pH 7 is relatively low. This indicates that the amount of N-CMC adsorbed on galena at pH 7 was much smaller than that at pH 10.

5.3.3.6. The N 1s spectrum of N-CMC treated galena at pH 10
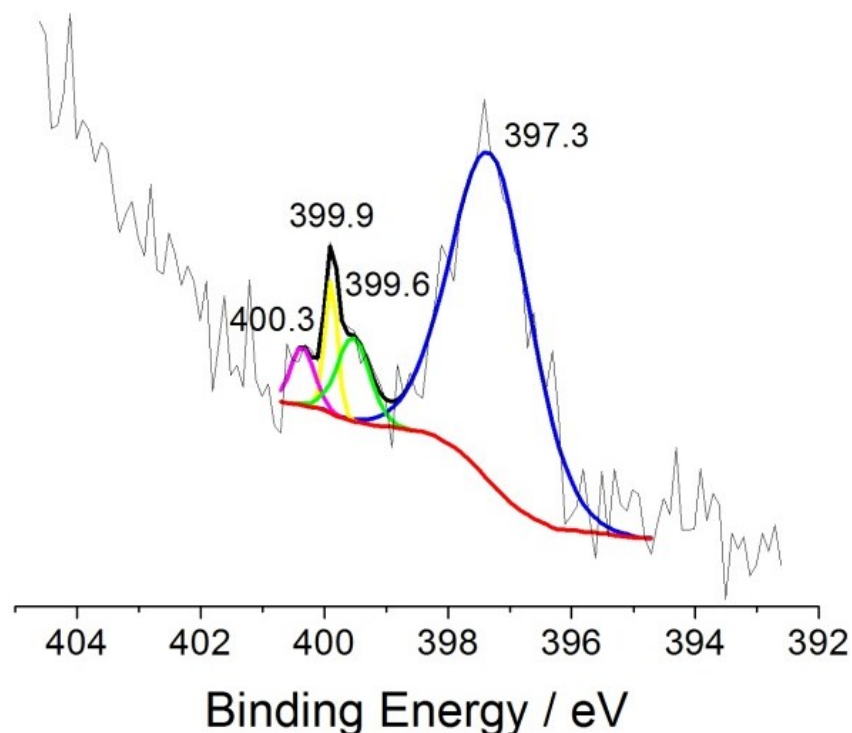
Figure 5.23 The resolved narrow scan N 1s spectrum of N-CMC on galena at pH 10

The N1s binding energy spectrum after treating galena with N-CMC is shown in Figure 5.23. As can be seen, the peak of $-NH-CH_2-COOH$ also stayed the same as at pH 7. The peak of $-NH-$ still did not shift, illustrating that no bonds were formed between Pb and $-COOH$. In addition to the peak at 400.3 eV which appeared on both spectra at pH 7 and at pH 10, another new peak at 399.9 eV also appeared at pH 10 with a relatively high intensity. The peaks at 400.3 eV and 399.9 eV are probably due to the N-Pb bonding with Pb at different valence states. Meanwhile, the total peak intensity is much higher than at pH 7 as mentioned before, indicating that more N-CMC was adsorbed on galena at pH 10.

5.3.3.7. Comparison between the spectra of chalcopyrite and galena

At pH 7, comparison of Figures 5.20 and 5.22 show that the N 1s binding energy in $-NH-$ and $-NH-CH_2-COOH$ shifted when N-CMC was reacted with chalcopyrite but it did not shift after reaction with galena. In addition, the overall binding energy peak intensity of N 1s on chalcopyrite is much higher than that on galena. Therefore, the adsorption of N-CMC on chalcopyrite was much stronger than on galena at pH 7. Furthermore, two types of

bonding were formed between N-CMC and chalcopyrite, through –NH– and –COOH, whereas for galena, no bond was formed between Pb and –COOH.

At pH 10, comparison of Figures 5.21 and 5.23 shows that although the N 1s binding energy peak shift and peak intensity on chalcopyrite were higher than those on galena, there was an extra N 1s binding energy peak with a high intensity on galena. Therefore, it is possible that the adsorption of N-CMC on galena was also strong at pH 10.

These analyses are consistent with the results of the flotation tests in that N-CMC exhibited a stronger depressing effect on chalcopyrite than galena at pH 7, while at pH 10 it showed little selectivity between chalcopyrite and galena.

5.3.4. Zeta potential measurements

Figure 5.24 shows the effects of pH and N-CMC's concentration on the zeta potential values of chalcopyrite and galena. The measurements were carried out using 10^{-2} M NaCl as an indifferent electrolyte. In the absence of N-CMC, both chalcopyrite and galena showed negative zeta potentials in the whole tested pH range, with projected isoelectric points (i.e.p.) lying somewhere between pH 2 and 3. Similar i.e.p. values for both chalcopyrite and galena were reported in the literature (Bebie et al., 1998; Rath & Subramanian, 1999). Due to the negative charge on both galena and chalcopyrite, a cationic depressant is supposed to be favored through electrostatic interaction. N-CMC is amphoteric in aqueous solutions: at low pH, the secondary amino groups on –NH-CH$_2$-COOH will be protonated, while at high pH, the –COOH group will lose a proton. Therefore, it can be cationic, electrically neutral or anionic depending on pH. The titration process of N-CMC can be expressed as the following formula based on the study by Wang et al. (2008):

$$R - NH_2{}^+ - CH_2 - COOH \xrightarrow{+ OH^-} R - NH_2{}^+ - CH_2 - COO^- \xrightarrow{+ OH^-} R - NH - CH_2 - COO^-$$
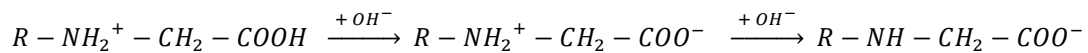
where R represents the glucose ring of N-CMC's structure.
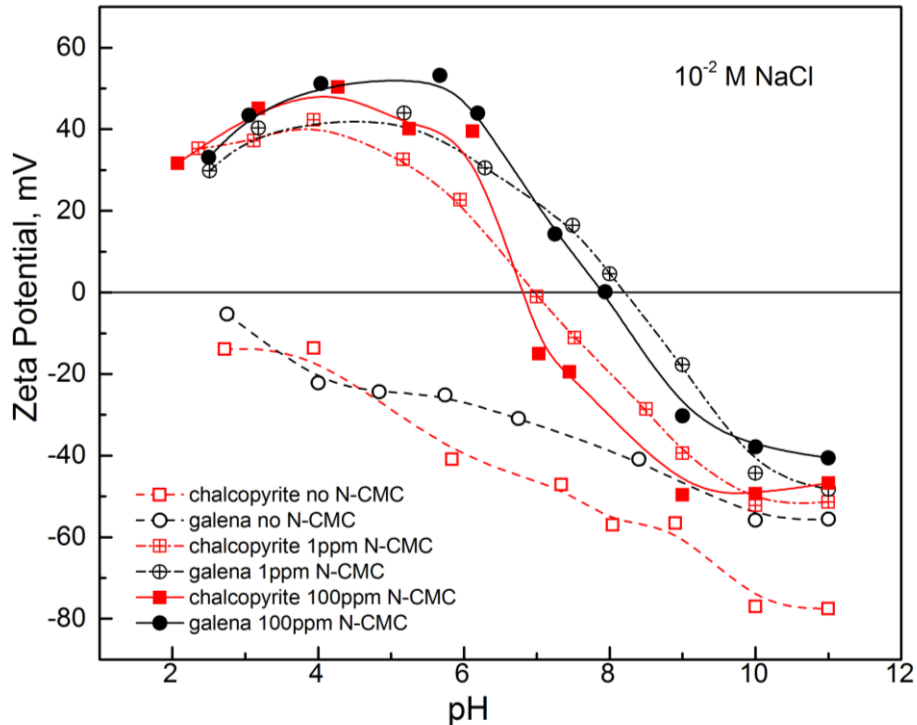
Figure 5.24 Zeta potentials of chalcopyrite and galena at different pH, with or without N-CMC

In the presence of 1 ppm N-CMC, the i.e.p. of chalcopyrite shifts to about pH 7 and the i.e.p. of galena shifts to around pH 8. The shifts of i.e.p. indicate that the adsorption of N-CMC happened on both chalcopyrite and galena. It can also be observed that the zeta potentials of both sulfide minerals were reversed at pH < i.e.p. after the addition of N-CMC. The positively charged N-CMC adsorbed on negatively charged mineral surfaces, and the positive charges on the Stern plane outnumbered the negative surface charge, thus leading to the reverse of zeta potential. The adsorption of N-CMC on chalcopyrite and galena at pH < i.e.p. can be partly attributed to the non-selective electrostatic attraction, and no evidence against chemical adsorption can be found from this experiment. At pH > i.e.p., both galena and chalcopyrite's zeta potentials are negative in the presence of 1 ppm N-CMC, but with a smaller magnitude than in the absence of N-CMC. The electrostatic attractions may still exist between N-CMC and both minerals, before the protonated secondary amino groups on N-CMC are neutralized. The decrease in the magnitude of zeta potential can be attributed to the offset of positively charged secondary amino groups on

N-CMC or due to the conformational rearrangement of electrically neutral N-CMC molecules adsorbed on mineral surfaces (Rath & Subramanian, 1999).

In the presence of 100 ppm N-CMC, the zeta potential – pH curves of both minerals are of similar shapes to those of 1 ppm N-CMC. Even though the concentration of N-CMC is 100 times higher, the zeta potentials of the two minerals are similar to those at 1 ppm N-CMC. It is reasonable to believe that the adsorption of N-CMC on both minerals was saturated at only 1 ppm N-CMC. This conclusion was also consistent with the result of single mineral flotation tests.

According to the zeta potential measurements, the secondary amino groups on N-CMC can adsorb on both galena and chalcopyrite through electrostatic attraction, but this interaction is non-selective and is ruled out as the reason for N-CMC's selectivity.

5.3.5. Summary

In the study of metal ion binding tests, N-CMC showed a stronger binding capacity with Cu^{2+} than with Pb^{2+}. The different depressant ability of N-CMC to chalcopyrite and galena was very possibly based on their affinities for the respective metal ions.

Based on the ToF-SIMS images and XPS analyses, it can be seen that N-CMC adsorbed mostly on chalcopyrite at pH 7 and the chemical bonds between N-CMC and chalcopyrite were stronger than galena. Meanwhile, the substituted –COOH groups played an important role in the selective depression of chalcopyrite at pH 7. Whereas at pH 10, although the affinity of N-CMC towards galena was not obvious from ToF-SIMS images, XPS measurements of the N 1s binding energies showed the formation of a relatively strong new bond between the N atom in N-CMC and the galena surface.

Zeta potential measurements showed electrostatic interaction between N-CMC and both chalcopyrite and galena. But this is not the reason for N-CMC's selectivity.

In general, the results of adsorption mechanism studies are consistent with the results from flotation tests in that N-CMC's depressant ability to chalcopyrite was much stronger than to galena at pH 7; while at pH 10, it depressed galena more than chalcopyrite but the selectivity was rather weak.

5.4. Mineral surface cleaning tests

In sulfide mineral flotation, it is known that the dissolved copper ions can adsorb on the surface of other sulfide minerals (Chandra & Gerson, 2009). The masking effect makes the separation of Cu-bearing minerals from other minerals difficult (Finkelstein, 1997). Often a surface cleaning agent, such as EDTA (ethylenediaminetetraacetic acid), needs to be used to clean the mineral surface (e.g., Wang & Forssberg, 1990). From the successful separation between chalcopyrite and galena conducted in this study, we believe that due to its strong binding capacity with copper ions, N-CMC may have a similar function as EDTA to remove the adsorbed copper ions from the surface of galena particles. A series of mineral surface cleaning tests were carried out to verify this assumption. The results are shown in Figure 5.25. This figure shows the copper ion concentrations detected in hydrochloric acid solution after using it to wash the Cu^{2+}-coated galena without ("Blank") or with prior treatment by N-CMC. As can be seen, much less copper ions were washed off by hydrochloric acid when the Cu^{2+}-coated galena was treated by N-CMC first. Therefore, N-CMC is capable of cleaning the galena surfaces of adsorbed copper ions.
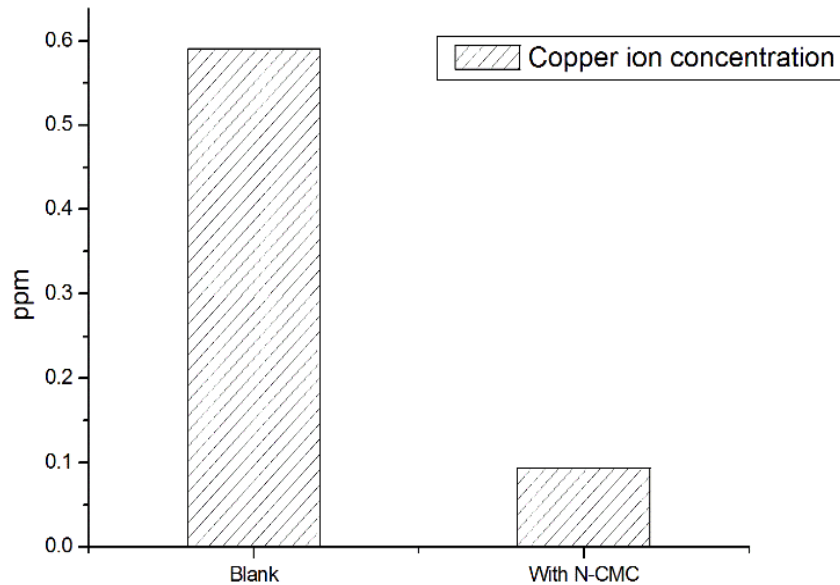
Figure 5.25 The concentration of copper ions released to HCl solution from Cu-coated galena sample. The Cu-coated galena sample was either treated with N-CMC ("With N-CMC") or not treated with N-CMC ("Blank") before being washed by the HCl solutions.
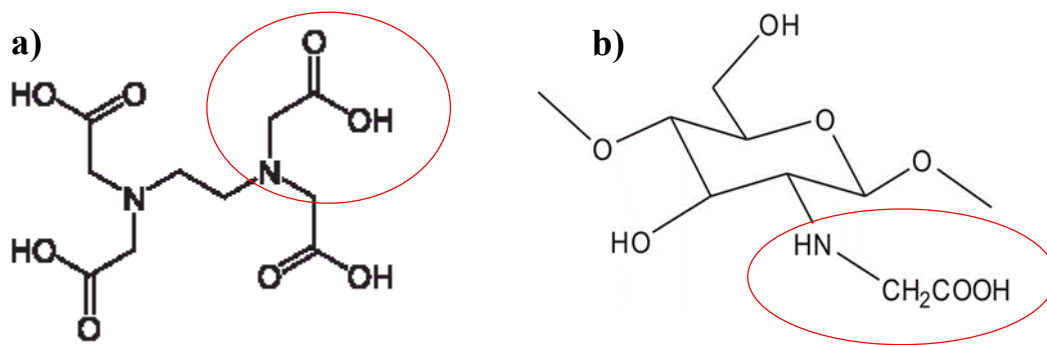
Figure 5.26 The N-C-C-O sequence in the structure of: a) EDTA; b) N-CMC.

According to Muzzarelli et al. (1982), the sequence of N-C-C-O in EDTA (shown as Figure 5.26a) which enables the formation of pertaatomic rings in metal chelates can also be found in N-CMC (shown as Figure 5.26b). This is probably the reason why N-CMC can function as a surface cleaning reagent as EDTA.

6. Conclusions

6.1. General findings

- Three carboxymethyl derivatives of chitosan were synthesized and their structures were confirmed by FTIR and NMR analyses. They were named as N-CMC, O-CMC and N-O-CMC with their amino groups on C-2, hydroxyl groups on C-6, and both amino and hydroxyl groups substituted by carboxymethyl groups, respectively. The solubility of these CMC products in aqueous solutions was in the order of N-CMC > N-O-CMC > O-CMC.

- N-CMC and N-O-CMC were tested as depressants in micro-flotation tests for chalcopyrite and galena with KEX as a collector. The selectivity of N-O-CMC was only observed in single mineral flotation but was absent in mixed mineral flotation tests. N-CMC showed a good selectivity in both single mineral and mixed mineral flotation tests, and it can depress chalcopyrite selectively under neutral pH without affecting the flotation of galena. At pH 10, galena was depressed by N-CMC and chalcopyrite can be floated.

- Only N-CMC was further studied in batch flotation tests following a bulk flotation and Cu-Pb differential flotation procedure. The test results indicated that N-CMC depressed chalcopyrite very well while allowing galena to be floated. The gap between their recoveries can be as high as 65 percentage points.

- As revealed by the adsorption mechanism studies, N-CMC had an affinity to Cu^{2+} ions over Pb^{2+} ions. At pH 7, N-CMC mainly adsorbed on chalcopyrite and the chemical bonds formed between chalcopyrite and N-CMC were stronger than the bonds between N-CMC and galena. At pH 10, the chemical interaction between N-CMC and galena may be slightly stronger than chalcopyrite, due to an extra bond formed between N and Pb. The electrostatic adsorption of N-CMC happened on both chalcopyrite and galena and it was not the reason for selectivity. Both –NH– (secondary amino) and –COOH groups were involved in the chemical and

electrostatic adsorption of N-CMC on chalcopyrite and galena, and the N-CMC's preference for chalcopyrite at pH 7 was mainly due to the –COOH group while the preference for galena at pH 10 was more likely due to the –NH– group.

- According to the mineral surface cleaning test results, N-CMC had the ability of removing adsorbed Cu^{2+} from the galena surface. This function is very similar to EDTA and may be attributed to the same sequence of N-C-C-O in their structures. With this function, N-CMC can separate Cu bearing sulfide minerals well from other sulfide minerals even when the mineral surfaces are cross-contaminated by various metal ions.

- In general, the selective depression and surface cleaning function make N-CMC a strong candidate to replace toxic depressants for the differential flotation of chalcopyrite and galena.

6.2. Suggested future work

In order to achieve a better understanding of N-CMC's adsorption behaviour on galena and chalcopyrite, the adsorption densities of N-CMC on both minerals are required to be studied with an increasing pH or increasing concentration of N-CMC.

Batch flotation tests were carried out in this study on mineral mixtures that were ground together. They are not sufficient as proof for N-CMC's effectiveness in industrial applications. Lab scale flotation tests using real ore samples mined from operating mines are very essential to further verify N-CMC's performance as a selective depressant.

The depressing effect of N-CMC was only studied on the differential flotation of chalcopyrite and galena in this work. Since N-CMC showed a stronger affinity on chalcopyrite, the separation between chalcopyrite and other sulfide minerals can also be expected. It is worthwhile to study the selectivity of N-CMC among different sulfide minerals.

The cleaning function of N-CMC to remove Cu^{2+} ions was only studied on galena's surface, and can be further investigated on sphalerite and other sulfide minerals. The experimental

procedures can also be redesigned since the method used in this study was not direct and convenient.

7. Appendix

7.1. Detailed procedures and raw data for batch flotation test

7.1.1. Test procedures

Table 7.1 Detailed procedures for batch flotation test

STAGE	TIME min	pH	ADDITION Reagent	ADDITION g/t	COMMENTS
Cu Pb Bulk Flotation					50 g chalcopyrite, 50 g galena, 300 g quartz grinding 30 seconds, 300 mL distilled water 400 g sample (dry basis) 1.5 L cell (bottom driven flotation machine, 900 rpm) Air flow rate: 7 L/min
Condition		10	10% NaOH		to pH 10.0
	3		KEX	25	5 mL KEX (2 g/L)
Cu Pb Bulk float 1	2	9.7	MIBC	1 drop	use if necessary
Condition		10	10% NaOH		to pH 10.0
	2		KEX	20	4 mL KEX (2 g/L)
Cu Pb Bulk float 2	2		MIBC	1 drop	use if necessary
Pb Flotation					Fine mineral from the Cu Pb Roughrt Flotation 1.5 L cell (bottom driven flotation machine, 900 rpm) Air flow rate: 7 L/min
Condition 1		10	10% NaOH		to pH 10.0

	3		N-CMC	40	8 mL N-CMC (2 g/L)
Pb float 1	1	10	MIBC	2 drop	use if necessary to white bubble rare out
Condition 2	3	10	N-CMC	10	2 mL N-CMC (2 g/L)
Pb float 2	1	10	MIBC	2 drop	use if necessary to white bubble rare out
Condition 3	3 3	10	N-CMC KEX	5 10	1 mL N-CMC (2 g/L) nothing can be floated out 2 mL KEX (2 g/L) but nothing can be floated out
		10 to 8			
Pb float 3	2	8	MIBC	2 drop	use if necessary to white bubble
Condition 4	3	10	KEX	10	2 mL KEX (2 g/L)
		10 to 8			
Pb float 4	1		MIBC	2 drop	use if necessary to white bubble
Condition 5	3 3	10	N-CMC KEX	5 5	1 mL N-CMC (2 g/L) 1 mL KEX (2 g/L)
		10 to 8			
Pb float 5	1	8	MIBC	2 drop	use if necessary
Condition 6	3 3	10	N-CMC KEX	5 5	1 mL N-CMC (2 g/L) 1 mL KEX (2 g/L) nothing can be floated out
		10 to 8			
	3 18	8	N-CMC KEX	5 65	1 mL N-CMC (2 g/L) 13 mL KEX (2 g/L)
		8 to 10			

				2 drop	use if necessary to white bubble
Pb float 6	2	10	MIBC	2 drop	use if necessary to white bubble
Condition 7	3	8	KEX	15	3 mL KEX (2 g/L)
		8 to 10			
Pb float 7	2	10	MIBC	2 drop	use if necessary to white bubble
Condition 8	3	8	KEX	15	3 mL KEX (2 g/L)
	3		N-CMC	10	2 mL N-CMC (2 g/L)
	12		KEX	90	16 mL KEX (2 g/L)
		8 to 10			
Pb float 8	2	10	MIBC	2 drop	use if necessary to white bubble

7.1.2. Metallurgical balance

Table 7.2 Raw data and calculations for bulk flotation

Product	Weight		Assay			Distribution (%)			
	(g)	(%)	Fe (%)	Pb (%)	Si (%)	Cu	Fe	Pb	Si
Pb conc 1	4.43	1.19	8.54	44.62	14.59	3.74	4.02	5.16	0.46
Pb conc 2	1.21	0.33	8.13	43.05	11.67	1.03	1.05	1.36	0.10
Pb conc 1+2	**5.64**	**1.51**	**8.45**	**44.28**	**13.96**	**4.77**	**5.06**	**6.52**	**0.56**
Pb conc 3	13.43	3.61	3.17	69.42	5.95	4.11	4.52	24.34	0.57
Pb conc 1+2+3	**19.07**	**5.12**	**4.73**	**61.99**	**8.32**	**8.89**	**9.59**	**30.86**	**1.13**
Pb conc 4	14.55	3.91	3.65	67.59	5.68	6.38	5.64	25.68	0.59
Pb conc 1+2+3+4	**33.62**	**9.03**	**4.26**	**64.41**	**7.18**	**15.27**	**15.23**	**56.54**	**1.72**
Pb conc 5	6.94	1.86	3.12	68.89	6.20	2.48	2.30	12.48	0.31
Pb conc 1+2+3+4+5	**40.56**	**10.90**	**4.07**	**65.18**	**7.01**	**17.75**	**17.53**	**69.02**	**2.03**
Pb conc 6	7.89	2.12	3.71	64.21	11.05	3.23	3.11	13.23	0.62
Pb conc 1+2+3+4+5+6	**48.45**	**13.01**	**4.01**	**65.02**	**7.67**	**20.99**	**20.64**	**82.25**	**2.65**
Pb conc 7	7.47	2.01	11.89	24.56	8.51	10.24	9.44	4.79	0.45
Pb conc 1-7	**55.92**	**15.02**	**5.06**	**59.62**	**7.78**	**31.23**	**30.07**	**87.04**	**3.11**
Pb conc 8	1.36	0.37	12.61	19.86	23.09	2.16	1.82	0.71	0.22
Pb conc 1-8	**57.28**	**15.39**	**5.24**	**58.67**	**8.14**	**33.38**	**31.89**	**87.75**	**3.33**
Pb flotation tail	26.50	7.12	15.81	6.82	17.05	52.80	44.51	4.72	3.23
Cu-Pb bulk conc	**83.78**	**22.50**	**8.58**	**42.27**	**10.96**	**86.18**	**76.40**	**92.47**	**6.56**
Cu Pb Bulk tail	288.50	77.50	0.77	1.00	45.37	13.82	23.60	7.53	93.44
Total	372.28	100.00	2.53	10.29	37.63	100.00	100.00	100.00	100.00
Measured			3.80	10.83	35.03				

Table 7.3 Raw data and calculations for Cu-Pb separation

Product	Weight		Assay			Distribution (%)			
	(g)	**(%)**	**Fe (%)**	**Pb (%)**	**Si (%)**	**Cu**	**Fe**	**Pb**	**Si**
Pb conc 1	4.43	5.29	8.54	44.62	14.59	4.34	5.26	5.58	7.04
Pb conc 2	1.21	1.44	8.13	43.05	11.67	1.19	1.37	1.47	1.54
Pb conc 1+2	**5.64**	**6.73**	**8.45**	**44.28**	**13.96**	**5.54**	**6.63**	**7.05**	**8.58**
Pb conc 3	13.43	16.03	3.17	69.42	5.95	4.77	5.92	26.33	8.70
Pb conc 1+2+3	**19.07**	**22.76**	**4.73**	**61.99**	**8.32**	**10.31**	**12.55**	**33.38**	**17.28**
Pb conc 4	14.55	17.37	3.65	67.59	5.68	7.41	7.38	27.77	9.00
Pb conc 1+2+3+4	**33.62**	**40.13**	**4.26**	**64.41**	**7.18**	**17.72**	**19.93**	**61.15**	**26.28**
Pb conc 5	6.94	8.28	3.12	68.89	6.20	2.88	3.01	13.50	4.69
Pb conc 1+2+3+4+5	**40.56**	**48.41**	**4.07**	**65.18**	**7.01**	**20.60**	**22.94**	**74.65**	**30.96**
Pb conc 6	7.89	9.42	3.71	64.21	11.05	3.75	4.07	14.31	9.49
Pb conc 1+2+3+4+5+6	**48.45**	**57.83**	**4.01**	**65.02**	**7.67**	**24.35**	**27.01**	**88.95**	**40.46**
Pb conc 7	7.47	8.92	11.89	24.56	8.51	11.88	12.35	5.18	6.92
Pb conc 1-7	**55.92**	**66.75**	**5.06**	**59.62**	**7.78**	**36.23**	**39.36**	**94.13**	**47.38**
Pb conc 8	1.36	1.62	12.61	19.86	23.09	2.50	2.38	0.76	3.42
Pb conc 1-8	**57.28**	**68.37**	**5.24**	**58.67**	**8.14**	**38.74**	**41.75**	**94.90**	**50.80**
Pb flotation tail	26.50	31.63	15.81	6.82	17.05	61.26	58.25	5.10	49.20
Cu Pb Bulk Conc Measured	83.78	100.00	8.58	42.27	10.96	100.00	100.00	100.00	100.00

7.2. Adsorption isotherm

Traditionally, in the process of determining the polysaccharides' adsorption isotherm, the concentration of polysaccharides in solution is measured as the determining parameter. By subtracting the residual amount of polysaccharides in solution from its total amount, the adsorbed amount of polysaccharides on mineral particles will be obtained. The most common methods of measuring the polysaccharides concentration are the DNS (3, 5-dinitrosalicylic aid) method (Miller, 1959) and the phenol-sulfuric acid method (Dubois et al.,1956). Both of them are based on the colors produced in the chemical reaction between

reducing sugar and phenol or 3, 5-dinitrosalicylic acid, and they both require colorimetric tests. However, by trial and error, the author found out neither of them can be used in determining the content of N-CMC. The detectable range in the DNS method is only from 200 ppm to 1000 ppm while the most interesting range for this study is below 100 ppm. Phenol-sulfuric acid has been successfully used in many tests for dextrin and starch, but the colours produced by N-CMC were too light to reveal any difference regardless of N-CMC's concentration. The reason for this phenomenon is still uncertain but it is very possible due to the unique structure of $NH-CH_2-COOH$ in N-CMC, which might disable the hydrolysis of N-CMC into reducing sugar.

Due to the failure of calorimetry methods, N-CMC's adsorption isotherm was then measured by the total carbon method. The amount of CO_2 produced by burning the N-CMC solution can provide an indirect hint for N-CMC's amount. However, the results obtained from this method are not very satisfactory. As can be seen from Figure 7.2 below, there is a drop for N-CMC's adsorption densities on both chalcopyrite and galena around 100 ppm which is hard to explain. In addition, as shown on Figure 7.3, the adsorbed amount of N-CMC on galena is higher than on chalcopyrite which is contradictory to the previous results. There are many possible reasons for the imperfect experiment results, including malfunction of the total carbon analyzer, carbon contamination from water or other sources, and the operating errors when picking up 200 μL samples, etc. Therefore, the adsorption isotherm experiment still requires further study by a new apparatus or repeated measurements, and can only be presented in the appendix as a reference.

7.2.1. Experimental procedures

As a function of pH and equilibrium N-CMC concentration, the adsorption densities of N-CMC on chalcopyrite and galena were studied. The concentration of N-CMC solution was determined by total carbon analysis, using the CM 5015 CO_2 coulometer together with the CM5300 furnace module from UIC Inc. The CO_2 coulometer can detect carbon in the range of 0.01 μg to 100 mg. A standard curve shown in Figure 7.1 was first drawn to figure out the linear relationship between the amount of carbon and the amount of N-CMC. And the linear equation was also calculated as: y=0.3035x-0.141.
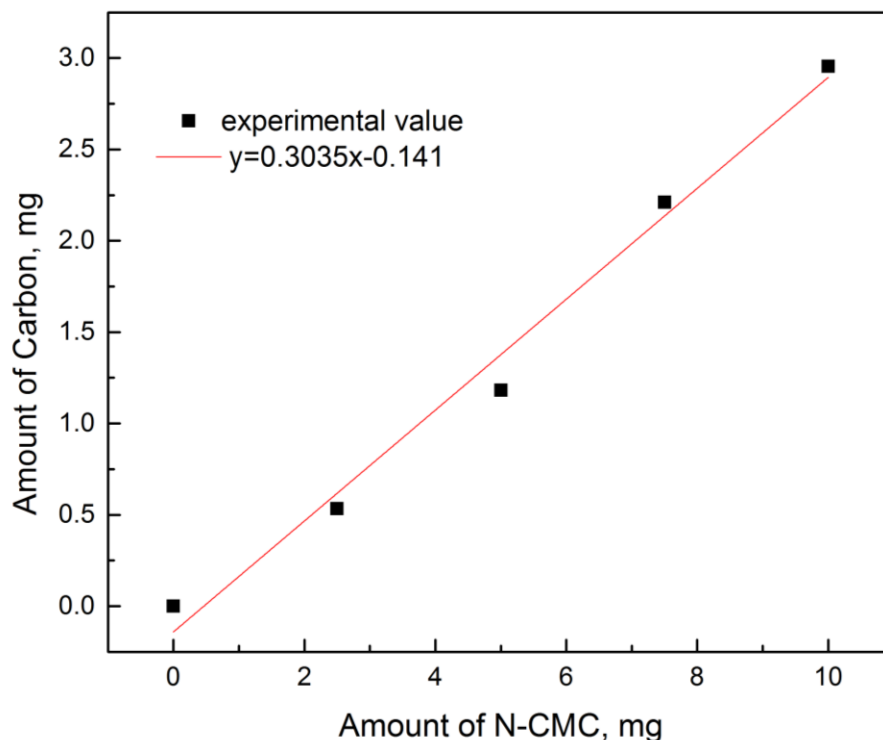
Figure 7.1 The standard curve

In the adsorption tests, 1 g of the -20 μm mineral powders were mixed with 50 mL of the N-CMC solution with a certain concentration. After the pH was adjusted and recorded, the suspension was then conditioned in a SI-600 shaking incubator (Jeio Tech, USA) for 30 minutes at 250 rpm, 25 ℃. After the conditioning, the solution pH was measured again and recorded. The suspension was then allowed to stand for a period until the supernatant was clear. 10 mL supernatant was taken as the sample, using a syringe with a 1 μm filter on the tip, and then stored in a sample bottle for carbon analysis.

In the carbon analysis, only 200 μL sample was measured each time. Each time before injecting a sample into the furnace, the system was allowed to purge for five minutes. The temperature of the furnace was set to 850 ℃ to thoroughly generate CO_2 from C in the sample. The result was shown as the amount of C and then translated in to the amount of N-CMC using the linear equation from above.

7.2.2. Results and discussion

The adsorption isotherms of N-CMC on chalcopyrite and galena at their natural pH are shown as Figure 7.2. The adsorption densities are presented per unit weight of minerals rather than per unit area. The adsorption isotherms of N-CMC on chalcopyrite and galena were similar. Both of them are shown as a high-affinity (a special Langmuir) type since they all reached the first maximum around a concentration of 60 ppm. A multilayer build-up appeared on both isotherms at higher N-CMC concentration. Overall, the adsorption densities of N-CMC on chalcopyrite were always higher than on galena.

To obtain the Langmuir equation of both isotherms, more data are required below 60 ppm.
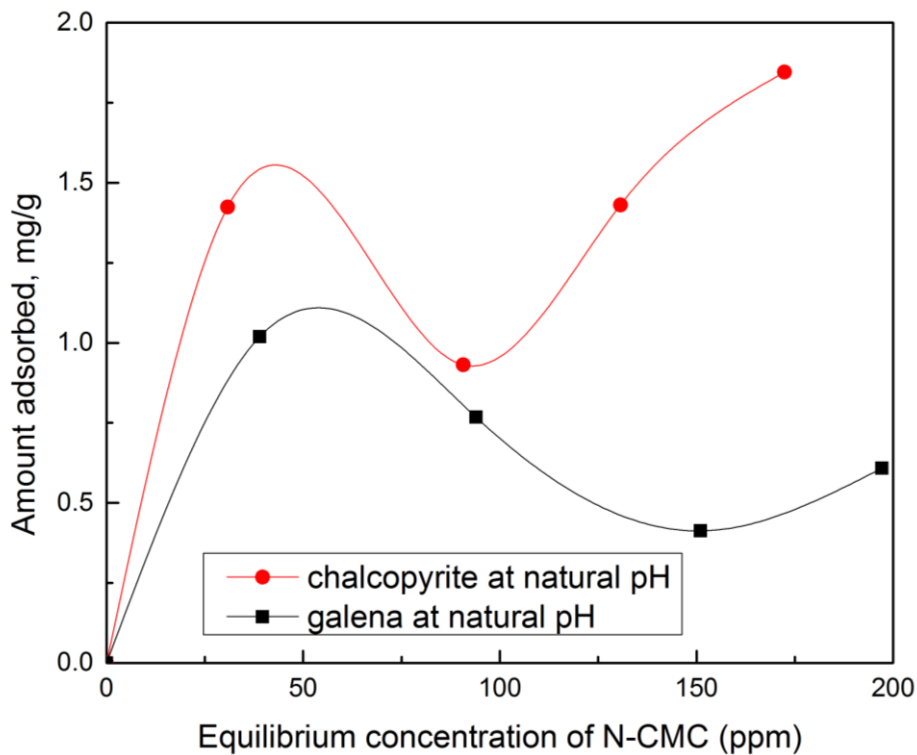
Figure 7.2 The adsorption isotherm (natural pH: 5.5-6.5, 25 ℃) of N-CMC on chalcopyrite and galena
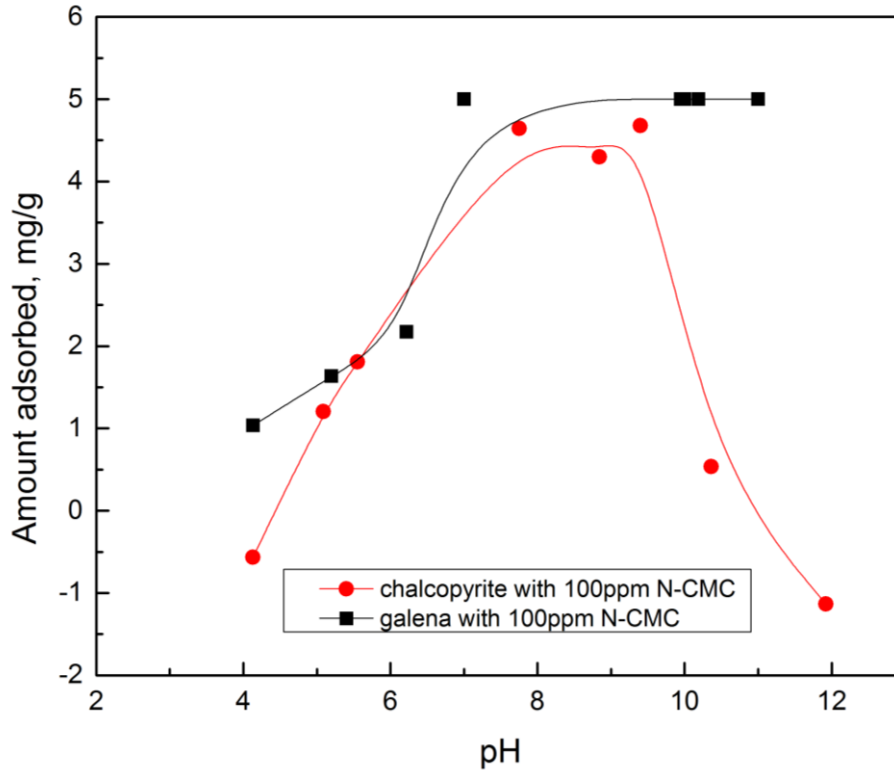
Figure 7.3 Effect of pH on the adsorption of N-CMC on chalcopyrite and galena with
100 ppm N-CMC

Figure 7.3 shows the adsorption of N-CMC on both minerals as a function of pH at 100 ppm of N-CMC. The adsorption density of N-CMC on galena increased with the pH and remained unchanged after reaching the maximum at pH 8. N-CMC's adsorption density on chalcopyrite reached its maximum at pH 7, while it was low (shown as minus 0 because of system errors) for both acidic and alkaline conditions. Both chalcopyrite and galena adsorbed most of the N-CMC at their i.e.p. values with N-CMC added. At natural pH (6-7), the adsorption density of N-CMC on chalcopyrite is slightly higher than on galena. Thus, it is possible that, N-CMC can depress chalcopyrite at natural pH while galena is floated. At pH 10, galena adsorbed almost all the N-CMC, while the adsorption density on chalcopyrite was barely above 0. This is also consistent with our flotation test result, that galena was depressed by N-CMC while chalcopyrite was floated at pH 10.

References

Afenya, P. M. (1982). Adsorption of xanthate and starch on synthetic graphite. *International Journal of Mineral Processing*, *9*(4), 303-319.

Allen, W., & Bourke, R. D. (1978). *Milling Practice in Canada. CIM Spec, 16,* 175.

Balajee, S. R., & Iwasaki, I. (1969). Adsorption mechanism of starches in flotation and flocculation of iron ores. *Trans. AIME*, *244*, 401-406.

Bakinov, K. G., Vaneev, I. I., Gorlovsky, S. I., Eropkin, U. I., Zashikhin, N. V., & Konev, A. S. (1964). *New methods of sulfide concentrate upgrading.* 7th International Mineral Processing Congress, New York, 227-238.

Beaussart, A., Mierczynska-Vasilev, A., & Beattie, D. A. (2009). Adsorption of dextrin on hydrophobic minerals. *Langmuir*, *25*(17), 9913-9921.

Bebie, J., Schoonen, M. A., Fuhrmann, M., & Strongin, D. R. (1998). Surface charge development on transition metal sulfides: an electrokinetic study. *Geochimica et Cosmochimica Acta*, *62*(4), 633-642.

Bhatnagar, A., & Sillanpää, M. (2009). Applications of chitin-and chitosan-derivatives for the detoxification of water and wastewater—a short review.*Advances in Colloid and Interface Science*, *152*(1), 26-38.

Bicak, O., Ekmekci, Z., Bradshaw, D. J., & Harris, P. J. (2007). Adsorption of guar gum and CMC on pyrite. *Minerals engineering*, *20*(10), 996-1002.

Blümich, B., Hagemeyer, A., Schaefer, D., Schmidt-Rohr, K., & Spiess, H. W. (1990). Solid State NMR spectroscopy in polymer science. *Advanced Materials*, *2*(2), 72-81.

Boulton, A., Fornasiero, D., & Ralston, J. (2003). Characterisation of sphalerite and pyrite flotation samples by XPS and ToF-SIMS. *International journal of mineral processing*, *70*(1), 205-219.

Brinen, J. S., & Reich, F. (1992). Static SIMS imaging of the adsorption of diisobutyl dithiophosphinate on galena surfaces. *Surface and interface analysis*, *18*(6), 448-452.

Brothers, R. (2002). Photometric Dispersion Analyzer THE PDA 2000 Operating Manual. *Cambridge, UK*.

Bulatovic, S., & Wyslouzil, D. M. (1995). Selection and evaluation of different depressants systems for flotation of complex sulphide ores. *Minerals engineering*, *8*(1), 63-76.

Bulatovic, S. M. (1999). Use of organic polymers in the flotation of polymetallic ores: A review. *Minerals engineering*, *12*(4), 341-354.

Bulatovic, S. M. (2007). *Handbook of flotation reagents: chemistry, theory and practice: volume 1: flotation of sulfide ores*. Elsevier.

Cao, M., & Liu, Q. (2006). Reexamining the functions of zinc sulfate as a selective depressant in differential sulfide flotation — the role of coagulation. *Journal of colloid and interface science*, *301*(2), 523-531.

Chandra, A. P., & Gerson, A. R. (2009). A review of the fundamental studies of the copper activation mechanisms for selective flotation of the sulfide minerals, sphalerite and pyrite. *Advances in Colloid and Interface Science*, *145*(1), 97-110.

Chattopadhyay, & D. P., Inamdar, M. S. (2014). Application of chitosan and its derivatives in Cu(II) ion removal from water used in textile wet processing. *Textile Research Journal*, *84*(14), 1539-1548.

Chen, L., Du, Y., & Zeng, X. (2003). Relationships between the molecular structure and moisture-absorption and moisture-retention abilities of carboxymethyl chitosan: II. Effect of degree of deacetylation and carboxymethylation. *Carbohydrate research*, *338*(4), 333-340.

Chen, R. N., Wang, G. M., Chen, C. H., Ho, H. O., & Sheu, M. T. (2006). Development of N,O-(carboxymethyl) chitosan/collagen matrixes as a wound dressing. *Biomacromolecules*, *7*(4), 1058-1064.

Chen, X. G., & Park, H. J. (2003). Chemical characteristics of *O*-carboxymethyl chitosans related to the preparation conditions. *Carbohydrate Polymers*, *53*(4), 355-359.

Cheng, H. N. (1984). Carbon-13 NMR analysis of ethylene-propylene rubbers. *Macromolecules*, *17*(10), 1950-1955.

Dash, M., Chiellini, F., Ottenbrite, R. M., & Chiellini, E. (2011). Chitosan—A versatile semi-synthetic polymer in biomedical applications. *Progress in Polymer Science*, *36*(8), 981-1014.

Delben, F., Muzzarelli, R. A., & Terbojevich, M. (1989). Thermodynamic study of the protonation and interaction with metal cations of three chitin derivatives. *Carbohydrate polymers, 11*(3), 205-219.

Delben, F., & Muzzarelli, R. A. (1989). Thermodynamic study of the interaction of *N*-Carboxymethyl chitosan with divalent metal ions. *Carbohydrate polymers*, *11*(3), 221-232.

Dobetti, L., & Delben, F. (1992). Binding of metal cations by N-carboxymethyl chitosans in water. *Carbohydrate polymers, 18*(4), 273-282.

Dolivo-Dobrovoskii, V.V., Rogachevskaya, T.A., (1957). *Depression action of some high-molecular organic compounds on sulfide minerals.* Obogashch. Rud 1, 30-40, CA 53:11135.

Domard, A., Gey, C., Rinaudo, M., & Terrassin, C. (1987). ^{13}C and ^{1}H nmr spectroscopy of chitosan and *N*-trimethyl chloride derivatives. *International Journal of Biological Macromolecules*, *9*(4), 233-237.

Dubois, M., Gilles, K. A., Hamilton, J. K., Rebers, P., & Smith, F. (1956). Colorimetric method for determination of sugars and related substances. *Analytical chemistry, 28*(3), 350-356.

Dutta, P. K., Dutta, J., & Tripathi, V. S. (2004). Chitin and chitosan: Chemistry, properties and applications. *Journal of Scientific and Industrial Research*, *63*(1), 20-31.

Dutta, P. K., Tripathi, S., Mehrotra, G. K., & Dutta, J. (2009). Perspectives for chitosan based antimicrobial films in food applications. *Food Chemistry*, *114*(4), 1173-1182.

Dybowski, C., Glatfelter, A., Cheng, H. N. (2010). ^{13}C NMR, Methods. *Encyclopedia of Spectroscopy and Spectrometry (Second Edition)*, 355-364.

Fairley, N. (2009). *CasaXPS manual 2.3. 15*. Acolyte Science.

Finkelstein, N. P. (1997). The activation of sulphide minerals for flotation: a review. *International Journal of Mineral Processing*, *52*(2), 81-120.

Fornasiero, D., & Ralston, J. (2006). Effect of surface oxide/hydroxide products on the collectorless flotation of copper-activated sphalerite. *International Journal of Mineral Processing*, *78*(4), 231-237.

Foster, J. F., Whistler, R. L., & Paschall, E. F. (1965). Starch: chemistry and technology. *Academic, New York*, 349.

Frahn, J. L., & Mills, J. A. (1959). Paper ionophoresis of carbohydrates. I. Procedures and results for four electrolytes. *Australian Journal of Chemistry*, *12*(1), 65-89.

Fuerstenau, D. W., & Fuerstenau, M. C. (1982). The flotation of oxide and silicate minerals. *Principles of flotation*, 109-158.

Fuerstenau, M. C., Miller, J. D., & Kuhn, M. C. (1985). *Chemistry of flotation*. Society for Mining Metallurgy.

Fuerstenau, D. W., Pradip, I. V. (2005). Zeta potentials in the flotation of oxide and silicate minerals. *Advances in Colloid and Interface Science*, *114*, 9-26.

Fuerstenau, M. C., Jameson, G. J., & Yoon, R. H. (Eds.). (2007). *Froth flotation: a century of innovation*. SME.

Grahame, D. C. (1947). The electrical double layer and the theory of electrocapillarity. *Chemical Reviews, 41*(3), 441-501.

Hanna, H. S. (1974). Adsorption of some starches on particles of spar minerals. In *Recent Advances in Science and Technology of Materials,* Springer US, 365-374.

Haung, H. H., Calara, J. V., Bauer, D. L., & Miller, J. D. (1978). Adsorption reactions in the depression of coal by organic colloids. *Recent Developments in Separation Science*, *4*, 115-133.

Hayes, E. R. (1986). *U.S. Patent No. 4,619,995*. Washington, DC: U.S. Patent and Trademark Office.

Hirano, S., Hirochi, K., Hayashi, K. I., Mikami, T., & Tachibana, H. (1991). Cosmetic and pharmaceutical uses of chitin and chitosan. In *Cosmetic and Pharmaceutical Applications of Polymers*, Springer US, 95-104.

Huang, P., Cao, M., & Liu, Q. (2012a). Using chitosan as a selective depressant in the differential flotation of Cu–Pb sulfides. *International Journal of Mineral Processing, 106,* 8-15.

Huang, P., Cao, M., & Liu, Q. (2012b). Adsorption of chitosan on chalcopyrite and galena from aqueous suspensions. *Colloids and Surfaces A: Physicochemical and Engineering Aspects*, *409*, 167-175.

Huang, P., Cao, M., & Liu, Q. (2013a). Selective depression of sphalerite by chitosan in differential PbZn flotation. *International Journal of Mineral Processing*, *122*, 29-35.

Huang, P., Cao, M., & Liu, Q. (2013b). Selective depression of pyrite with chitosan in Pb–Fe sulfide flotation. *Minerals Engineering*, *46*, 45-51.

Israelachvili, J. N. (2011). *Intermolecular and surface forces: revised third edition*. Academic press.

Jayakumar, R., Prabaharan, M., Nair, S. V., Tokura, S., Tamura, H., & Selvamurugan, N. (2010). Novel carboxymethyl derivatives of chitin and chitosan materials and their biomedical applications. *Progress in Materials Science, 55*(7), 675-709.

Jenkins, P., & Ralston, J. (1998). The adsorption of a polysaccharide at the talc–aqueous solution interface. *Colloids and Surfaces A: Physicochemical and Engineering Aspects*, *139*(1), 27-40.

Jin, R., Hu, W., & Meng, S. (1987). Flotation of sphalerite from galena with sodium carboxymethyl cellulose as a depressant. *Mineral and Metall Process*, *4*, 227-232.

Juang, R. S., Wu, F. C., & Tseng, R. L. (1999). Adsorption removal of copper (II) using chitosan from simulated rinse solutions containing chelating agents. *Water Research, 33*(10), 2403-2409.

Khosla, N. K., Bhagat, R. P., Gandhi, K. S., & Biswas, A. K. (1984). Calorimetric and other interaction studies on mineral—starch adsorption systems. *Colloids and surfaces*, *8*(4), 321-336.

Kittur, F. S., Harish Prashanth, K. V., Udaya Sankar, K., & Tharanathan, R. N. (2002). Characterization of chitin, chitosan and their carboxymethyl derivatives by differential scanning calorimetry. *Carbohydrate polymers*, *49*(2), 185-193.

Kong, X. (2012). Simultaneous determination of degree of deacetylation, degree of substitution and distribution fraction of –COONa in carboxymethyl chitosan by potentiometric titration. *Carbohydrate Polymers*, *88*(1), 336-341.

Larkin, P. (2011). *Infrared and Raman spectroscopy; principles and spectral interpretation*. Elsevier.

Laskowski, J. S., Liu, Q., & Bolin, N. J. (1991). Polysaccharides in flotation of sulphides. Part I. Adsorption of polysaccharides onto mineral surfaces. *International journal of mineral processing*, *33*(1), 223-234.

Lee, V. F. F. (1974). *Solution and shear properties of chitin and chitosan* (Doctoral dissertation, University of Washington.).

Lin, K.F., Burdick, C.L. (1988). Polymeric depressants. In: Somasundaran, P., Moudgil, B.M. (Eds.), *Reagents in Mineral Technology*. Marcel Dekker, New York, pp. 471–483.

Liu, Q., & Laskowski, J. S. (1989a). The role of metal hydroxides at mineral surfaces in dextrin adsorption, II. Chalcopyrite-galena separations in the presence of dextrin. *International Journal of Mineral Processing*, 27(1), 147-155.

Liu, Q., & Laskowski, J. S. (1989b). The interactions between dextrin and metal hydroxides in aqueous solutions. *Journal of Colloid and Interface Science*, *130*(1), 101-111.

Liu, Q., Zhang, Y., & Laskowski, J. S. (2000). The adsorption of polysaccharides onto mineral surfaces: an acid/base interaction. *International Journal of Mineral Processing*, *60*(3), 229-245.

Liu, Q., & Laskowski, J. S. (2002). Adsorption of polysaccharides on mineral surfaces from aqueous solutions. In *Encyclopedia of Surface and Colloid Science (Arthur Hubbard, Ed.),* Marcel Dekker, 573-590.

Miller, G. L. (1959). Use of DNS reagent for the measurement of reducing sugar. *Analytical Chemistry, 31*(1), 426-428.

Miller, J. D., Laskowski, J. S., & Chang, S. S. (1983). Dextrin adsorption by oxidized coal. *Colloids and surfaces*, *8*(2), 137-151.

Morni, N. M., & Arof, A. K. (1999). Chitosan–lithium triflate electrolyte in secondary lithium cells. *Journal of power sources*, *77*(1), 42-48.

Morris, G. E., Fornasiero, D., & Ralston, J. (2002). Polymer depressants at the talc–water interface: adsorption isotherm, microflotation and electrokinetic studies. *International Journal of Mineral Processing*, *67*(1), 211-227.

Moulder, J. F., Stickle, W. F., Sobol, P. E., & Bomben, K. D. (1992). *Handbook of X-ray photoelectron spectroscopy* (Vol. 40). Eden Prairie, MN: Perkin Elmer.

Mourya, V. K., Inamdar, N. N., & Tiwari, A. (2010). Carboxymethyl chitosan and its applications. *Advanced Materials Letters*, *1*(1), 11-33.

Muzzarelli, R. A., Tanfani, F., Emanuelli, M., & Mariotti, S. (1982). *N*-(carboxymethylidene) chitosans and *N*-(carboxymethyl) chitosans: Novel chelating polyampholytes obtained from chitosan glyoxylate. *Carbohydrate Research, 107*(2), 199-214.

Muzzarelli, R. A., Lough, C., & Emanuelli, M. (1987). The molecular weight of chitosans studied by laser light-scattering. *Carbohydrate research*, *164*, 433-442.

Muzzarelli, R. A. (1988). Carboxymethylated chitins and chitosans. *Carbohydrate polymers, 8*(1), 1-21.

Nieto, J. M., Peniche-Covas, C., & Del Bosque, J. (1992). Preparation and characterization of a chitosan-Fe (III) complex. *Carbohydrate polymers*, *18*(3), 221-224.

Némethy, G., & Scheraga, H. A. (1962). Structure of water and hydrophobic bonding in proteins. I. A model for the thermodynamic properties of liquid water. *The Journal of Chemical Physics*, *36*(12), 3382-3400.

Ogawa, K., Oka, K., & Yui, T. (1993). X-ray study of chitosan-transition metal complexes. *Chemistry of materials*, *5*(5), 726-728.

Okuyama, K., Noguchi, K., Kanenari, M., Egawa, T., Osawa, K., & Ogawa, K. (2000). Structural diversity of chitosan and its complexes. *Carbohydrate Polymers*, *41*(3), 237-247.

Pearse, M. J. (2005). An overview of the use of chemical reagents in mineral processing. *Minerals Engineering*, *18*(2), 139-149.

Pearson, F. G., Marchessault, R. H., & Liang, C. Y. (1960). Infrared spectra of crystalline polysaccharides. V. Chitin. *Journal of Polymer Science*, *43*(141), 101-116.

Pillari, C. K. S., Paul, W., & Sharma, C. P. (2011). Chitosan: manufacture, properties and uses. In *Chitosan: Manufacture, Properties and Usage (Samuel P. Davis, Ed.),* Nova Science Publisher, 133-215.

Pugh, R. J. (1989a). Macromolecular organic depressants in sulphide flotation—a review, 1. Principles, types and applications. *International Journal of Mineral Processing*, *25*(1), 101-130.

Rath, R. K., & Subramanian, S. (1999). Adsorption, electrokinetic and differential flotation studies on sphalerite and galena using dextrin. *International journal of mineral processing, 57*(4), 265-283.

Ravi Kumar, M. N. (2000). A review of chitin and chitosan applications. *Reactive and functional polymers*, *46*(1), 1-27.

Rinaudo, M., Dung, P. L., Gey, C., & Milas, M. (1992). Substituent distribution on *O, N*-carboxymethylchitosans by ^{1}H and ^{13}C nmr. *International journal of biological macromolecules*, *14*(3), 122-128.

Sahu, S. K., Maiti, S., Maiti, T. K., Ghosh, S. K., & Pramanik, P. (2011). Hydrophobically modified carboxymethyl chitosan nanoparticles targeted delivery of paclitaxel. *Journal of drug targeting*, *19*(2), 104-113.

Schnarr, J. R. (1978). Brunswick mining and smelting corporation. *Milling Practice in Canada. CIM Spec, 16,* 158-161.

Shahidi, F., Arachchi, J. K. V., & Jeon, Y. J. (1999). Food applications of chitin and chitosans. *Trends in Food Science & Technology*, *10*(2), 37-51.

Siwek, B., Zembala, M., & Pomianowski, A. (1981). A method for determination of fine-particle flotability. *International Journal of Mineral Processing*, *8*(1), 85-88.

Somasundaran, P. (1969). Adsorption of starch and oleate and interaction between them on calcite in aqueous solutions. *Journal of Colloid and Interface Science*, *31*(4), 557-565.

Somasundaran, P., & Wang, D. (2006). *Solution chemistry: minerals and reagents* (Vol. 17). Elsevier.

Stowe, K. G., Chryssoulis, S. L., & Kim, J. Y. (1995). Mapping of composition of mineral surfaces by TOF-SIMS. *Minerals engineering*, *8*(4), 421-430.

Subban, R. H. Y., Arof, A. K., & Radhakrishna, S. (1996). Polymer batteries with chitosan electrolyte mixed with sodium perchlorate. *Materials Science and Engineering: B*, *38*(1), 156-160.

Taylor, T. G., & Iddies, H. A. (1926). Separation of the amyloses in some common starches. *Industrial & Engineering Chemistry*, *18*(7), 713-717.

Thermo Nicolet Corporation (2001). Introduction to Fourier Transform Infrared Spectrometry, *Retrieved from Thermo Nicolet Corporation website*: *<http://mmrc.caltech.edu/FTIR/FTIRintro.pdf>*.

Tiwary, A. K., Sapra, B., Kaur, G., & Rana, V. (2011). Chitosan: manufacture, properties and uses. In *Chitosan: Manufacture, Properties and Usage (Samuel P. Davis, Ed.),* Nova Science Publisher, 71-131.

Tungtong, S., Okonogi, S., Chowwanapoonpohn, S., Phutdhawong, W., & Yotsawimonwat, S. (2012). Solubility, viscosity and rheological properties of water-soluble chitosan derivatives. *Maejo International Journal of Science and Technology, 6*(02), 315-322.

Upadhyaya, L., Singh, J., Agarwal, V., & Tewari, R. P. (2013). Biomedical applications of carboxymethyl chitosans. *Carbohydrate polymers*, *91*(1), 452-466.

Varma, A. J., Deshpande, S. V., & Kennedy, J. F. (2004). Metal complexation by chitosan and its derivatives: a review. *Carbohydrate Polymers*, *55*(1), 77-93.

Wagner, C. D., Powell, C. J., Allison, J. W., & Rumble, J. R. (1997). NIST X-ray Photoelectron Spectroscopy Database (Version 2.0). *Retrieved from NIST Standard Reference Data Program website: <http://www.nist.gov/srd>*.

Wan Ngah, W. S., Teong, L. C., & Hanafiah, M. A. K. M. (2011). Adsorption of dyes and heavy metal ions by chitosan composites: A review. *Carbohydrate Polymers*, *83*(4), 1446-1456.

Wang, K., & Liu, Q. (2013). Adsorption of phosphorylated chitosan on mineral surfaces. *Colloids and Surfaces A: Physicochemical and Engineering Aspects*, *436*, 656-663.

Wang, L. C., Chen, X. G., Liu, C. S., Li, P. W., & Zhou, Y. M. (2008). Dissociation behaviors of carboxyl and amine groups on carboxymethyl-chitosan in aqueous system. *Journal of Polymer Science Part B: Polymer Physics*, *46*(14), 1419-1429.

Wang, M., Xu, L., Zhai, M., Peng, J., Li, J., & Wei, G. (2008). γ-ray radiation-induced synthesis and Fe (III) ion adsorption of carboxymethylated chitosan hydrogels. *Carbohydrate polymers*, *74*(3), 498-503.

Wang, X., & Forssberg, E. (1990). EDTA-induced flotation of sulfide minerals. *Journal of colloid and interface science*, *140*(1), 217-226.

Weisseborn, P. K., Warren, L. J., & Dunn, J. G. (1995). Selective flocculation of ultrafine iron ore. 1. Mechanism of adsorption of starch onto hematite. *Colloids and surfaces A: Physicochemical and engineering aspects*, *99*(1), 11-27.

Wie, J., & Fuerstenau, D. W. (1974). The effect of dextrin on surface properties and the flotation of molybdenite. *International Journal of Mineral Processing*, *1*(1), 17-32.

Wills, B. A., & Napier-Munn, T. (2006). *Wills' mineral processing technology: an introduction to the practical aspects of ore treatment and mineral recovery*. Butterworth-Heinemann.

Yue, L., Zhang, L., & Zhong, H. (2014). Carboxymethyl chitosan: A new water soluble binder for Si anode of Li-ion batteries. *Journal of Power Sources*, *247*, 327-331.

Zeng, D., Wu, J., & Kennedy, J. F. (2008). Application of a chitosan flocculant to water treatment. *Carbohydrate polymers*, *71*(1), 135-139.